

# TiDES - Young Supernova Selection Pipeline

Harry Addison<sup>1</sup> , Chris Frohmaier<sup>2</sup> , Kate Maguire<sup>3</sup> , Robert C. Nichol<sup>1</sup>, Isobel Hook<sup>4</sup> ,  
Stephen J. Smartt<sup>5,6</sup> 

<sup>1</sup>*Department of Physics, University of Surrey, Guildford GU2 7XH, United Kingdom*

<sup>2</sup>*School of Physics and Astronomy, University of Southampton, Southampton SO17 1BJ, United Kingdom*

<sup>3</sup>*School of Physics, Trinity College Dublin, The University of Dublin, Dublin 2, Ireland*

<sup>4</sup>*Department of Physics, Lancaster University, Lancaster, Lancashire LA1 4YB, UK*

<sup>5</sup>*Department of Physics, University of Oxford, Keble Road, Oxford, OX1 3RH, UK*

<sup>6</sup>*Astrophysics Research Centre, School of Mathematics and Physics, Queen's University Belfast, BT7 1NN, UK*

Accepted XXX. Received YYY; in original form ZZZ

## ABSTRACT

Early-time spectroscopy of supernovae (SNe), acquired within days of explosion, yields crucial insights into their outermost ejecta layers, facilitating the study of their environments, progenitor systems, and explosion mechanisms. Recent efforts in early discovery and follow-up of SNe have shown the potential insights that can be gained from early-time spectra. The Time-Domain Extragalactic Survey (TiDES), conducted with the 4-meter Multi-Object Spectroscopic Telescope (4MOST), will provide spectroscopic follow-up of transients discovered by the Legacy Survey of Space and Time (LSST). Current simulations indicate that early-time spectroscopic studies conducted with TiDES data will be limited by the current SN selection criteria. To enhance TiDES's capability for early-time SN spectroscopic studies, we propose an additional set of selection criteria focusing on early-time (young) SNe (YSNe). Utilising the Zwicky Transient Facility live transient alerts, we developed criteria to select YSNe while minimising the sample's contamination rate to 28 percent. The developed criteria were applied to LSST simulations, yielding a sample of 1167 Deep Drilling Field survey SNe and 67388 Wide Fast Deep survey SNe for follow-up with 4MOST. We demonstrate that our criteria enables the selection of SNe at early-times, enhancing TiDES's future early-time spectroscopic SN studies. Finally, we investigated 4MOST-like observing strategies to increase the sample of spectroscopically observed YSNe. We propose that a 4MOST-like observing strategy that follows LSST with a delay of 3 days is optimal for the TiDES SN survey, while a 1 day delay is most optimal for enhancing the early-time science in conjunction with our YSN selection criteria.

**Key words:** surveys – transients: supernovae – techniques: photometric – techniques: spectroscopic

## 1 INTRODUCTION

Supernovae (SNe) are a diverse set of transients with many different progenitor scenarios and explosion mechanisms. For the case of thermonuclear (Type Ia) supernovae, there are two traditional progenitor scenarios (single-degenerate scenario [Whelan & Iben \(1973\)](#) and double-degenerate scenario [Iben & Tutukov \(1984\)](#)), while there are many different explosion mechanisms being studied, which include double-detonation models ([Fink et al. 2007, 2010](#); [Kromer et al. 2010](#); [Shen & Moore 2014](#); [Polin et al. 2019](#); [Magee et al. 2021](#); [Boos et al. 2024](#)), core-degenerate explosions ([Soker 2011](#); [Wang et al. 2016](#)), triple collision models ([Kushnir et al. 2013](#); [Hallakoun & Maoz 2019](#)), and rotating super-Chandrasekhar mass explosions ([Stefano et al. 2011](#)).

To investigate the explosion mechanisms of SNe Ia, previous studies have investigated the early light curves of SN Ia events ([Riess et al. 1999](#); [Hayden et al. 2010](#); [Ganeshalingam et al. 2011](#); [Firth et al. 2014](#); [Deckers et al. 2022](#)). In addition to early-time photometry, early-time spectroscopy can further provide us with a wealth of information about the explosion dynamics. Spectra taken within

a few days of explosion allow us to trace the outermost layers of the ejecta. From these spectra we can determine the chemical abundances of the outer layers, which can then be used to distinguish between explosion models ([Magee et al. 2021](#); [Ogawa et al. 2023](#)).

Furthermore, early-time spectra are not only useful for studying thermonuclear SN explosion mechanisms, but they can also be used to study core collapse (CC) SNe. Early-time spectra can be used to investigate the progenitor systems of CC SNe by providing us with the ability to constrain the progenitor's chemical abundance, wind speed, and mass loss ([Pastorello et al. 2007](#); [Smith et al. 2007](#); [Smith et al. 2023](#); [Zimmerman et al. 2024](#)). They can also be used to study SNe that display a “bump” in their pre-peak light curves, which is thought to result from an interaction of the shock front with circumstellar material (CSM; [Piro & Morozova 2016](#); [Gagliano et al. 2022](#); [Kozyreva et al. 2022](#)), a binary companion ([Kasen 2009](#)), or from the presence of short-lived radioactive isotopes ([Noebauer et al. 2017](#)).

Besides the study of SN progenitors and explosion mechanisms, early-time spectra can also be very useful for classifications. Some types of SNe, such as stripped envelope SN that retain a small hydrogen envelope, can only be reliably classified from their early phase spectra ([Dong et al. 2023](#)). Additionally, the ability to spectro-

\* E-mail: ha00871@surrey.ac.uk

scopically classify SNe early in their evolution allows us to conduct targeted observations of high interest SNe, such as the previously mentioned “bump” SNe or other peculiar types.

Currently, our spectroscopic samples of SNe, and in particular early-time spectra, are restricted by the availability of spectroscopic resources that can quickly follow-up photometrically discovered transients. The *Zwicky Transient Facility* (ZTF; Bellm et al. 2018; Masci et al. 2018) is one of the leading facilities of transient astronomy, with its Northern Sky Survey observing the northern sky (declination  $> -31^\circ$ ) every 3 days in both the  $g$ - and  $r$ -bands. This has allowed for the discovery of many transient events, however, a key part of ZTF’s success is its *Bright Transient Survey* (BTS; Fremling et al. 2020). BTS uses an automated low resolution integral field unit spectrograph, the Spectral Energy Distribution Machine (Ben-Ami et al. 2012; Blagorodnova et al. 2018; Rigault et al. 2019), to complement the Northern Sky Survey by providing spectroscopic follow-up of the ZTF discovered transients. The main aim of BTS is to provide a complete sample of spectroscopically classified extra-galactic transients within the Northern Sky Survey that are brighter than 18.5 mag (Fremling et al. 2020). Since June 2018, ZTF and BTS have found and spectroscopically classified over 9500 SNe<sup>1</sup>.

In the coming years the detection rates of transients will be greatly increased, with the Vera C. Rubin Observatory’s *Legacy Survey of Space and Time* (LSST; Ivezić et al. 2019) discovering millions of SNe. Along with increased photometric observations of SNe, we will also see a large increase in our spectroscopic SN samples. The *Time-Domain Extragalactic Survey* (TiDES; Swann et al. 2019, Frohmaier et al. in prep.) is one of the twenty five surveys to be conducted on the 4 metre *Multi-Object Spectroscopic Telescope* (4MOST; de Jong et al. 2019), providing follow-up spectra of LSST transients. TiDES will operate over 5 years in parallel with the other 4MOST surveys, constructing the largest spectroscopic cosmological SN sample to date (Frohmaier et al. in prep., hereafter CF).

In order to obtain follow-up spectra of LSST transients, TiDES will select its targets by applying sets of selection criteria to the real time transient alerts that LSST will send out (CF). The different sets of selection criteria will be used in conjunction with one another to enhance the scientific output of TiDES. The current proposed selection criteria for SN are described by CF, and are as follows:

- Transient detected to  $> 5\sigma$  in three or more bands.
- Transient observed on two distinct nights.
- Transient is brighter than 22.5 mag in any  $griz$  filter.

Using simulations of LSST and 4MOST, CF showed that their current SN selection criteria predominantly selects pre-peak SNe from the LSST alerts. However, they also showed that there is on average a seven-day delay between the selection of a target from LSST and its subsequent follow-up using 4MOST. This results in many of the obtained SN spectra being taken during post-peak SN phases, with very few spectra obtained for phases (relative to peak brightness hereafter) before  $-15$  days. Therefore, studies such as that of SN explosion mechanisms, progenitor compositions, wind speeds, mass loss, and early-time CSM/binary companion interactions will be limited with the TiDES spectroscopic SN sample based on current plans.

In this study, we propose a new set of selection criteria for TiDES that are focused on selecting transients as early as possible for the purpose of producing a SN sample for early-time astrophysical stud-

ies. Our criteria are designed to be used in conjunction with the other selection criteria implemented within TiDES, specifically focusing on enhancing the TiDES sample of early-time SN spectra. Whilst early triggering is our primary objective, our selection criteria must also ensure that the young SN (YSN) sample is not highly contaminated. This is due to TiDES having a limited number of fibre hours that we do not want to waste on non-real sources. By using the ZTF live transient alerts and LSST simulations, we aim to demonstrate that our proposed selection criteria will provide TiDES with more early-time SN targets to follow-up with 4MOST than the current selection criteria, whilst minimising the contamination.

Additionally, we investigate observing strategies with the aim of optimising the 4MOST observing strategy for the use case of the TiDES SN survey and our YSN selection criteria. We explore different observing strategies to improve the quality of the obtained SN spectra, also considering the need for a quick follow-up of the targets in order to make full use of the early SN triggers provided by our YSN selection criteria. We do not consider the impact that the investigated observing strategies have on the other 4MOST surveys when determining an optimal strategy. In this work our objective is not to produce a full observing strategy for 4MOST, but rather to provide guidelines for future works towards developing and simulating the 4MOST observing strategy.

This paper is organised as follows: in Section 2 we present the development of our YSN selection criteria using the ZTF live transient alerts. In Section 3, we adapt and apply our developed selection criteria to an LSST simulation, presenting the resulting YSN sample. The YSN sample is then evaluated by comparing it to the SN sample produced by the current TiDES selection criteria. In Section 4, we investigate different 4MOST observing strategies, attempting to optimise the output of the TiDES survey and our YSN selection criteria. Finally, in Section 5 we summarise the conclusions of this study.

## 2 YSN SELECTION CRITERIA DEVELOPMENT

TiDES will obtain its targets from the live transient alerts that LSST will produce. As LSST is expected to see first light in 2025<sup>2</sup>, we must look to other means of developing and testing our selection criteria. One way in which this could be done is with the LSST simulations such as those used by CF, which simulate a SN population and their LSST photometric observations. However, one major limitation of these simulations is that they focus on the extragalactic Universe, excluding Galactic events (such as cataclysmic variables) that form a major source of contamination for a young and bright extragalactic transient search. Therefore, the LSST simulations used by CF do not fully represent the transient/variable sky that will be present in the live LSST transient alerts. As we want to produce a high purity (low contamination) YSN sample, as to not waste TiDES’s allocated fibre hours on non-real sources, using the LSST simulations alone is not enough to investigate this requirement. Therefore, we made use of the ZTF live transient alerts, which will be similar to the LSST alerts, to develop and investigate suitable selection criteria that produce a high purity YSN sample.

<sup>1</sup> ZTF Bright Transient Survey, <https://sites.astro.caltech.edu/ztf/bts/bts.php> (accessed 29/08/2024)

<sup>2</sup> LSST project status, available at <https://www.lsst.org/about/project-status> (accessed 17/10/2024)

## 2.1 Proposed YSN Selection Criteria

ZTF observes the sky with a cadence of two to three days in the  $g$ - and  $r$ -filter bands (Fremling et al. 2020). When a source is detected to vary above a specified detection threshold in the difference image, an alert is sent out to the wider community through brokers (Patterson et al. 2018). These alerts contain information about the source including, but not limited to; its object ID, coordinates, magnitude and filter band, associated detections from the last 30 days, and cutouts of science and difference images. Additionally, brokers provide their own data products to enhance the ZTF alerts. For example, the Lasair broker (Smith et al. 2019; Williams et al. 2024) supplies a contextual classification of the object using its contextual classifier, Sherlock (Young 2023). In this study we adopted Lasair as our broker of choice, which is predominantly motivated by its use by TiDES for development purposes.

We considered the information provided in the ZTF alerts, along with additional data products provided by Lasair, and proposed a set of YSN selection criteria. These proposed criteria are presented in Table 1 along with a summary of the motivations behind using them, which are discussed in more detail below.

Our first proposed criterion, objects must be brighter than 22.5 mag in either the  $r$ - or  $g$ -band, was adopted from the current TiDES selection criteria. CF used this to ensure that a selected object is bright enough to meet the TiDES SN spectral success criteria (SSC), which is a criterion that defines whether or not an observation was successful. The SSC for TiDES SN is that for a given spectrum the mean signal to noise ratio in the wavelength range 4500 – 8000Å is more than 5 per 15 Å, which is based on the ability of SN classification tools to provide reliable classifications (CF). Therefore, we also require our objects to be brighter than 22.5 mag. It is worth mentioning that ZTF has a best case  $5\sigma$  limit of  $\sim 21.5$  mag (Bellm et al. 2018), meaning that this criterion has no effect on the produced ZTF SN samples.

The second criterion, that objects must have a declination between  $-5^\circ$  and  $70^\circ$ , was implemented to mimic the 4MOST declination range, which is from  $-70^\circ$  to  $5^\circ$ . As the ZTF and 4MOST footprints are predominantly in the Northern and Southern hemispheres respectively, there is very little footprint overlap between the surveys. Therefore, we made the decision to shift the 4MOST declination range Northward by  $65^\circ$ , which puts the declination range ( $-5^\circ < \text{declination} < 70^\circ$ ) in the ZTF footprint but covers a similar area to that of 4MOST footprint.

Our next criterion, exclusion of objects between Galactic latitudes of  $-10^\circ$  and  $10^\circ$ , was used to remove the Galactic plane from our selection region. As TiDES is an extragalactic survey, we are only interested in extragalactic transients. Therefore, this criteria reduces the number of Galactic transients that are selected by our selection criteria.

The fourth criterion, an object must have two or more positive difference detections greater than  $5\sigma$  in the same band, is to exclude objects with a single or no positive detections in both the  $g$ - and  $r$ -bands. As is made clear in Section 2.2, by applying this criterion we reduced the computational resources and time required to apply our last two criteria.

Next we utilised Sherlock (Young 2023), a contextual classifier, to filter out objects that we considered as contamination such as: variable stars (VS), active galactic nuclei (AGN), cataclysmic variables (CV), and bright stars (BS). The classifier is not 100 percent accurate, but we are not looking for a complete sample of YSNs, and our last two selection criteria are focused on removing any contaminants that remain.

Our penultimate criterion, referred to as the age constraint, is a constraint on the time since the first detection of an object. This was utilised to reduce the contamination of our selected YSN sample by removing long-lived transients. The age constraint should also reduce the number of post peak SNe in the sample as it will remove SN that have been observed over longer periods of time, which are likely no longer early-time SNe. Unlike the previous criteria, the age criterion does not have a clear definitive threshold value, so we tested two values: 7 and 14 days.

Our final criterion, a brightening rate constraint, was used to further remove contaminants from our YSN sample. As the brightening rate of a SN in its early phases is generally much more rapid than at near-peak phases, we exploited this property to filter out “slowly” brightening and dimming sources that are unlikely to be linked to the early phases of a SN outburst. To employ this criterion, we used equation 1 to calculate the brightening rate between the latest observation and the mean of the second latest night’s observations of the same filter band.

$$\text{Brightening rate} = \frac{-(m_{\text{latest}} - m_{\text{night2}})}{\text{JD}_{\text{latest}} - \text{JD}_{\text{night2}}} \quad (1)$$

where the brightening rate is in units of magnitudes per day (mag/day),  $m_{\text{latest}}$  is the apparent magnitude of the latest observation,  $m_{\text{night2}}$  is the mean magnitude of the previous available night’s observations in the same filter band as the latest observation,  $\text{JD}_{\text{latest}}$  is the Julian date (JD) of the latest observation, and  $\text{JD}_{\text{night2}}$  is the average JD of the previous available night’s observations in the same filter band as the latest observation. We associate a positive brightening rate with a source that is brightening, hence the use of the negative magnitude difference between the two nights ( $m_{\text{latest}} - m_{\text{night2}}$ ) in equation 1. We compared the latest observation to the observations from the previous available night, as observations (of the same band) taken within the same night can vary in magnitude (but within error), which in some cases can cause a false sense of brightening or dimming between the consecutive observations. For the same reason, we took the mean of the  $g$ - or  $r$ -band observations on the previous available night.

As with the age criterion, the brightening rate does not have a definitive threshold value, and so we applied and tested three values: 0.05 mag/day, 0.1 mag/day, and 0.2 mag/day. For an object to be selected as a YSN, it had to have a brightening rate more positive than the mentioned values, which corresponds to a more rapid brightening than the threshold values.

## 2.2 Querying Lasair for Transient Data

In order to choose the most suitable values for the age and brightening rate criteria, as well as to evaluate our proposed YSN selection criteria, we produced YSN samples by applying our criteria to the ZTF live transient alerts.

To apply the age and brightening rate criteria, we obtained the light curves of the objects that resulted from our Lasair filters. This was achieved by using the light curve query method within Lasair’s Python API, which allows you to download the full light curve (detections and non-detections) of an object using its ZTF candidate ID. We then calculated the “age” of the object and applied the age constraint to it, producing an “age” restricted sample. For this sample of objects, the brightening rate was then calculated and the brightening rate criterion was applied to produce a YSN sample.

**Table 1.** Developed YSN selection criteria for use on the ZTF live transient alerts. Provided are the criteria along with a description of each criterion’s purpose. \* This criterion has no effect when applied to ZTF live transient alerts as ZTF only detects objects brighter than 21.5 mag. \*\* The multiple values provided are the values that were tested, and only one value for a given criterion was applied at any given time.

Criterion	Reasoning
$g$ - or $r$ - band magnitude $< 22.5$ mag *	Ensures that the object will meet the TiDES SN SSC
$-5^\circ < \text{Declination} < 70^\circ$	Simulate extent of 4MOST declination range
Galactic latitude $< -10^\circ$ OR Galactic latitude $> 10^\circ$	Removal of Galactic transient sources
Number of $g$ - or $r$ -band $> 5\sigma$ positive difference detections $\geq 2$	Two or more $> 5\sigma$ $g$ - or $r$ -band detections required for brightening rate criterion
Sherlock classification not: VS, AGN, CV, BS	Removal of contaminants
Age $< 7, 14$ days **	Removes older objects that are unlikely pre-peak SNe
Brightening rate $> 0.2, 0.1, 0.05$ mag/day **	Removes dimming and slow brightening sources that are unlikely to be YSNs.

### 2.3 YSN Selection Criteria Testing

Throughout the development of our YSN selection criteria, several different YSN samples were produced to test the different proposed age and brightening rate threshold values. A sample was also produced with the purpose of evaluating our finalised selection criteria. The details of how these YSN samples were produced, along with discussions of these samples for the purpose of development and evaluation of our criteria are provided in the sections that follow, with a summary provided in Figure 1.

#### 2.3.1 Selection of Age Criterion Threshold

To select a suitable constraint value for the ambiguous age criterion, we first produced samples of objects by applying the methods outlined in Section 2.2 to the ZTF alerts over a period of two weeks (5<sup>th</sup> July 2023 - 19<sup>th</sup> July 2023). A two week time span was used as it provided a large enough sample to provide a relatively quick insight into the different sets of selection criteria that were tested. For the purpose of selecting a suitable age constraint, the brightening rate criterion was not applied. As mentioned in Section 2.1, we tested two threshold values (7 and 14 days) for the age criterion, and so two samples were produced.

To select the more optimised constraint value for our needs, we investigated the contamination (non-YSN objects) of the samples. This was accomplished by cross matching the objects to the *Transient Name Server* (TNS; IAU 2023), obtaining their classifications if possible. We conducted the cross-matching approximately one month after the two-week period, which allowed time for the classification of the newly discovered objects. For the TNS classified SNe, we visually inspected their light curves to determine an estimate of their peak  $g$ -band brightness JD, or if not possible their  $r$ -band peak brightness JD. This was to separate out the pre- and post-peak SNe, the latter of which are considered contaminants in this study.

Presented in Table 2 are the TNS classifications for the two samples that we produced for the two values of the age criterion. As is shown in Table 2, the age constraint value of 7 days selected 40 pre-peak SNe and rejected 13. It is also shown that the criteria with a 7 days age constraint selected 6009 objects that are considered as contaminants (post-peak SNe, AGN, CV, Tidal disruption event (TDE), and long blue variables (LBV)) and potential contaminants (unclassified objects), while it rejected 1933 contaminants and potential contaminants. This equates to the produced sample having a completeness of 75 percent (40/53 pre-peak SNe). Meanwhile the sample has a potential contamination, percentage of selected objects that are non pre-peak SNe to the total number of selected objects, of 99.34 percent (6009 contaminants and potential contaminants / 6049

**Table 2.** TNS classifications of the objects that passed and failed the selection criteria stated in Table 1 with the exception of the brightening rate criterion.

Classification	Age $< 14$ days		Age $< 7$ days	
	Pass Criteria	Fail Criteria	Pass Criteria	Fail Criteria
Pre-peak SNe	53	0	40	13
Post-peak SNe	14	151	6	159
AGN	0	7	0	7
CV	0	6	0	6
TDE	1	2	1	2
LBV	0	1	0	1
Unclassified	6201	1559	6002	1758

total selected objects). Although this sample’s potential contamination is extremely high, in the sections that follow (Sections 2.3.2 and 2.3.3) we demonstrate that the brightening rate (which is not applied to this sample) further reduces the contamination. We also discuss the assumption that all of the unclassified objects in the sample are contaminants, which may not be the case.

For the age constraint value of 14 days, from Table 2 it can be seen that 53 pre-peak SNe were selected and none were rejected, while 6216 and 1726 contaminants (post-peak SNe, AGN, CV, TDE, and LBV) and potential contaminants (unclassified objects) were selected and rejected respectively. Although the selection criteria selected all of the available pre-peak SNe, the sample that passed the criteria is up to 99.15 percent contaminated (6216 contaminants and potential contaminants / 6269 total selected objects). As with the previous sample, we note that the potential contamination is very high and that we later address this with the application of the brightening rate criterion and a discussion of the unclassified objects.

The aim for our selection criteria is to produce a high purity sample of YSNs. However, as both of the age constraint values tested produced samples with approximately the same potential contamination (~99 percent), we decided to select the age threshold value based on the completeness of the sample. As the 14 day criterion value has a higher completeness compared to that of the 7 day constraint value, 100 percent compared to 75 percent respectively, we choose to use the 14 day threshold for our finalised selection criteria.

#### 2.3.2 Selection of Brightening Rate Criterion Threshold

As the exact brightening rate criterion is also not well physically motivated, we produced three YSN samples for the three different brightening rate criterion threshold values (0.05, 0.1, 0.2 mag/day). The samples were produced using the methods outlined in Section 2.2, adopting the previously determined age criterion threshold value

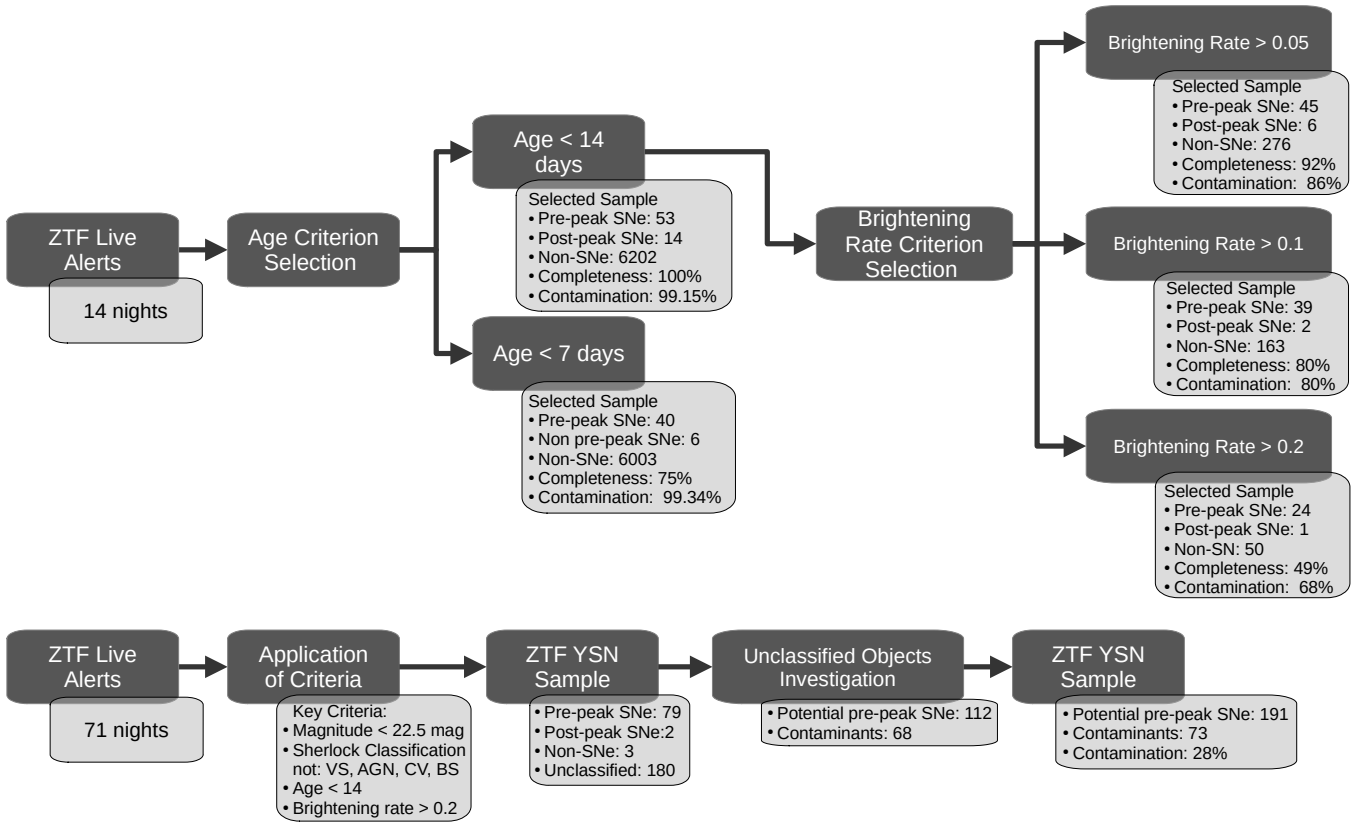


**Figure 1.** Summary of the development process and the produced YSN samples. (Upper flow chart) Overview of the samples used to determine suitable age and brightening rate criteria threshold values. (Lower flow chart) Summary of the ZTF sample used to evaluate the YSN selection criteria with the chosen age and brightening rate criteria thresholds of 14 days and 0.2 mag/day respectively.

of 14 days and the three different brightening rate criterion values to be tested. As with the age criterion determination (see Section 2.3.1), we analysed the potential contamination of the samples, obtaining the TNS classifications of the objects as well as the date of peak brightness for the TNS SNe to further classify them as pre- or post-peak SNe at the time of selection.

Presented in Table 3 are the TNS classifications for the three samples that were produced by each of the different brightening rate criterion threshold values (0.05, 0.1, 0.2 mag/day). From the Table it is shown that the brightening rate criterion threshold value of 0.05 mag/day produced a YSN sample with a completeness of 92 percent (45 selected pre-peak SNe / 49 total pre-peak SNe) that is up to 86 percent contaminated (282 contaminants and potential contaminants / 327 total selected objects). The sample produced from the brightening rate threshold of 0.1 mag/day is 80 percent complete (ratio of selected to total pre-peak SNe) with a potential contamination of 80 percent (ratio of selected non pre-peak SNe to all selected objects). The final YSN sample, produced from a threshold of 0.2 mag/day, has a completeness and potential contamination of 49 percent and 68 percent, respectively.

As the focus for our YSN selection criteria is to produce a high purity YSN sample, we decided to use the 0.2 mag/day threshold for our finalised selection criteria. This is because the 0.2 mag/day threshold produced a sample with a potential contamination of 68.00 percent, whereas the other thresholds produced samples that were up to 10 percent more contaminated. Although the threshold value of 0.2 mag/day produced the purest sample, its potential contamination is

still quite high at 68.00 percent. We further discuss the contamination level of the produced YSN sample in Sections 2.3.3 and 3.3. Finally, we note that the sample produced using the 0.2 mag/day threshold has the lowest completeness of the three YSN samples. However, the completeness of the sample is not the focus of the YSN selection criteria and therefore, is of less concern in this study.

### 2.3.3 Evaluation of Selection Criteria

With values for the ambiguous criteria values determined, we further investigated the performance of our selection criteria. For this purpose, we collected an additional two months (56 nights) of detections (26<sup>th</sup> September - 20<sup>th</sup> November 2023) and combined it with our initial two week sample, creating a sample of ZTF live transients (taken over 71 nights) that we tested our selection criteria on. Evaluation of our YSN criteria was accomplished following the methods outlined in Section 2.2, applying the criteria stated in Table 1 with the age criterion value of 14 days and the brightening rate criterion value of 0.2 mag/day.

To examine the performance of our selection criteria, we first examined how well the produced YSN sample meets our aim of not being over contaminated. Up until this point, we have treated the unclassified objects as potential contamination, however, some of these objects may not be contaminants. As such, we investigated the apparent contaminating sources by visually inspecting their light curves, in an attempt to understand their nature and why they were selected. This was not a feasible task to do for all of our previously

**Table 3.** Three samples of objects that pass or failed the selection criteria stated in Table 1, where we adopted an age criterion value of 14 days and applied three different brightening rate thresholds (0.05 mag/day, 0.1 mag/day, and 0.2 mag/day). Provided are the TNS classifications of the objects, with the SNe being further classified based on if they were pre-peak or post-peak at the time of selection or rejection.

Classification	Brightening Rate > 0.05 mag/day		Brightening Rate > 0.1 mag/day		Brightening Rate > 0.2 mag/day	
	Pass Criteria	Fail Criteria	Pass Criteria	Fail Criteria	Pass Criteria	Fail Criteria
Pre-peak SNe	45	4	39	10	24	25
Post-peak SNe	6	11	2	15	1	16
TDE	1	0	1	0	1	0
Unclassified	275	5926	162	6039	49	6152

**Table 4.** TNS classifications of the selected (passed criteria) and rejected (failed criteria) objects in the dataset collected by applying our determined optimal selection criteria (see Table 1, and Sections 2.3.1 and 2.3.2) to 71 nights of ZTF live transient alerts.

Classification	Passed Criteria	Failed Criteria
Pre-peak SNe	79	74
Post-peak SNe	2	81
AGN	0	2
CV	1	14
TDE	1	1
Variable Star	0	2
Nova	1	0
Unclassified	180	7556

investigated samples due to number of unclassified objects within them.

Presented in Table 4 is the produced YSN sample covering 71 nights of ZTF data, which shows that there are 79 pre-peak SNe, 2 post-peak SNe, 1 CV, 1 TDE, 1 Nova, and 180 unclassified objects that pass our criteria. Investigating the 180 unclassified objects further, through visually inspecting their light curves, we believe that at least 112 of the 180 unclassified sources are pre-peak selected SNe. When visually inspecting the light curves we considered the shape, rise, time-scales, and evolution of the light curve to determine if it was SN-like. We then estimated the date of peak brightness in the *g*-band (if available, else the *r*-band) to see if our selection criteria had selected the object pre- or post-peak. Presented in Figure 2 are light curves of three examples of likely SNe from the unclassified objects, while Figure 3 shows examples of light curves of contaminants that were selected by our criteria. Some of the contaminants are likely unclassified variable stars (see left and middle plots of Figure 3), while the nature of the remaining contaminants is unknown (see right plot of Figure 3). As 112 of the 180 unclassified objects are likely pre-peak SNe, the number of pre-peak SNe in our sample is 191, while the number of contaminants is reduced to 73. Therefore, the contamination of the produced YSN sample is approximately 28 percent (73 contaminants / 264 total objects).

At a first glance, a YSN sample with a contamination rate of 28 percent might seem to be too high to be worth implementing into TiDES. However, this percentage does not quantify the number of fibre hours that TiDES would spend on the YSN sample contaminants. By calculating the wasted fibre hours as a percentage of TiDES’s total fibre hours we can evaluate if this contamination level is too high or not. While we can calculate the number of fibre hours that would be wasted based on our ZTF YSN sample, this would not be representative of the actual number that would be wasted during the operation of 4MOST/TiDES. This is because TiDES, and hence our selection

criteria, will be selecting objects from LSST as opposed to ZTF. LSST will produce a much larger YSN sample than that produced from the ZTF alerts. Therefore, we revisit this discussion of wasted fibre hours in Section 3.3.3, where we used the LSST simulations to produce a YSN sample.

In addition to investigating the contamination of our YSN sample, we also evaluated our selection criteria’s performance by analysing its ability to select YSNs. This was achieved by investigating the phases at which the TNS classified SNe were selected from the ZTF live transient alerts. To calculate the phase at which a SN was selected, we used its estimated peak brightness JD and the JD of the observation from which the SNe were first selected.

Presented in Figure 4 is the resulting selection phase distribution of the SNe in our YSN sample. It can be seen that the phase distribution peak is at a phase of  $-7$  days and extends down to a phase of  $-18$  days. Furthermore, it can be seen that the two post-peak SNe that were selected have phases less than two days. It is possible that the two post-peak selected SNe are actually pre-peak selected SNe. The maximum two day shift in the peak brightness date needed to define these post-peak SNe as pre-peak SNe could be accounted for by the visually inspected peak brightness date estimates.

The resulting phase distribution of the TNS classified SNe in our YSN demonstrates that our YSN selection criteria is selecting pre-peak SNe as intended, with 50 SNe (62 percent of the sample) being selected before a phase of  $-6$  days. It should be noted that the presented phases are not definitive phases and may not represent the true phase distribution of the SNe due to several caveats. Firstly, the phases are calculated from estimates of the light curves’ peak date, which were determined by visual inspection of the SN light curves. Secondly, the phases are calculated using the peak date of the *g*-band light curve (where possible), and so when comparing to a trigger based on an *r*-band observation this could induce an error into the estimated trigger phase. Lastly, the phases presented are of TNS classified SNe only, which means that these objects were selected for follow-up observations in order to provide the spectroscopic classification. Therefore, this could have introduced a selection effect on the triggered SNe phases. Despite these caveats, our results are promising. However, to fully evaluate our YSN selection criteria’s performance we need to investigate how they perform when applied to LSST, which we present in Section 3.

### 3 APPLICATION OF YSN SELECTION CRITERIA TO LSST

To investigate the impact that our YSN selection criteria could have on the TiDES transient programme, we can not use the ZTF live alerts as they are not fully representative of the future LSST alerts that TiDES will draw its targets from. Some of the differences between the two

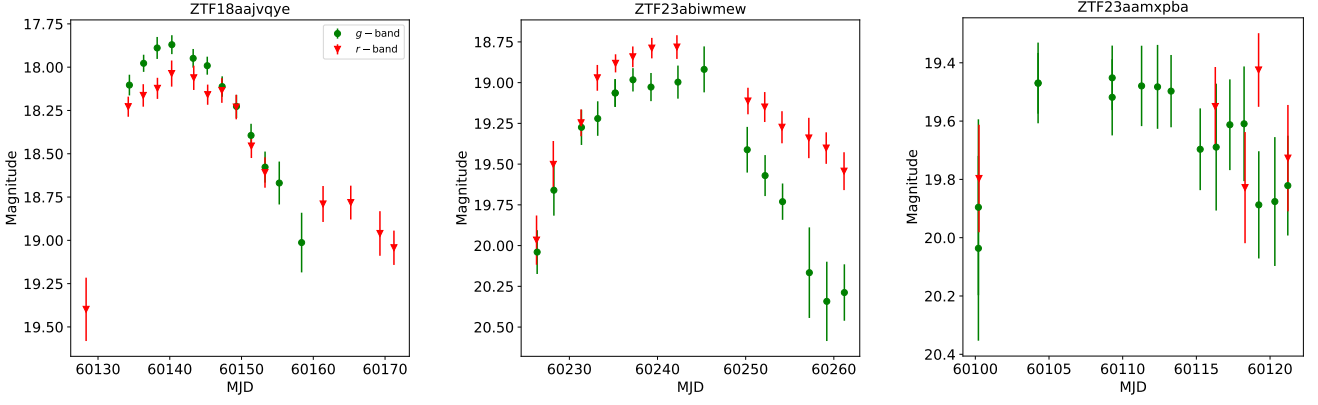


**Figure 2.** Light curves ( $g$ - and  $r$ -bands) of potential SNe from the unclassified objects in our ZTF selected YSN sample. These objects were identified as potential SNe due to their timescales, shape, rise, and evolution being comparable to known classified SNe.

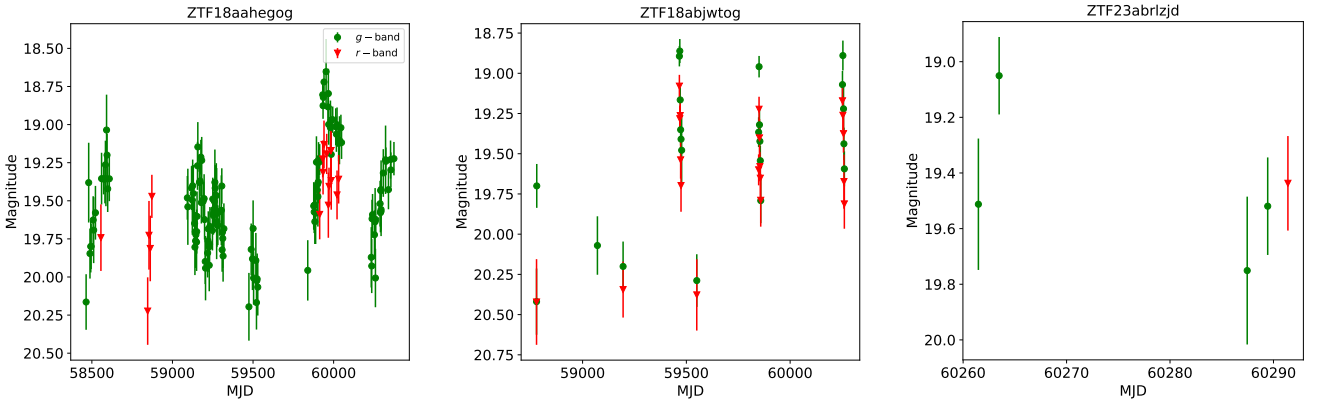


**Figure 3.** Light curves of unclassified contaminants in our YSN sample selected from the ZTF live transient alerts. (Left and middle)  $g$ - and  $r$ -band light curves of unclassified objects in our sample that are variable in nature over a long period of time. They are likely to be variable stars that have not yet been classified. (Right)  $g$ - and  $r$ -band light curves of an unclassified object in our sample that has no clear nature.

surveys that will affect our selection criteria and the resulting objects are as follows: LSST has different filter bands ( $ugrizY$ -bands), LSST has a much fainter limiting magnitude than ZTF, and LSST will have a different observing strategy to that of ZTF. With this in mind, we adapted the ZTF developed YSN selection criteria for use with LSST data, evaluating their performance by applying them to the LSST simulation used by CF.

### 3.1 Producing a LSST YSN Sample

#### 3.1.1 Adaptation of ZTF Developed YSN Selection Criteria

With the addition of the  $i$ -,  $z$ -,  $u$ -, and  $Y$ -bands of LSST, we adapted the ZTF developed YSN selection criteria by including the LSST  $i$ - and  $z$ -bands. We do not include the  $u$ - and  $Y$ -bands in our selection criteria as these bands are not often used by LSST and so our selection criteria will not benefit from including them. To incorporate the  $i$ - and  $z$ -bands in our selection criteria, we included them in our applied magnitude criterion, as well as adapting our age and brightening rate criteria so that observations in the  $i$ - and  $z$ -bands are also considered if available. Additionally, we alter the declination range to that of 4MOST ( $-70^\circ < \text{Dec} < 5^\circ$ ), however, we do not alter the excluded Galactic coordinates as we still want to remove the Galactic plane. The adapted YSN selection criteria for LSST are stated, with reasoning, in Table 5.

We applied our LSST based selection criteria, stated in Table 5, to the LSST Wide Fast Deep (WFD) survey and the Deep Drilling Fields (DDF) survey, which we discuss further in Section 3.1.2. It is worth noting that we made use of an LSST simulation, meaning that we could not apply the Sherlock classification criterion stated in Table 5 as it is only available through the Lasair broker. Regardless, we state this criterion in the table as it should be applied to the future LSST live transient alerts to help exclude contamination from our YSN sample.

#### 3.1.2 Applying the Selection Criteria

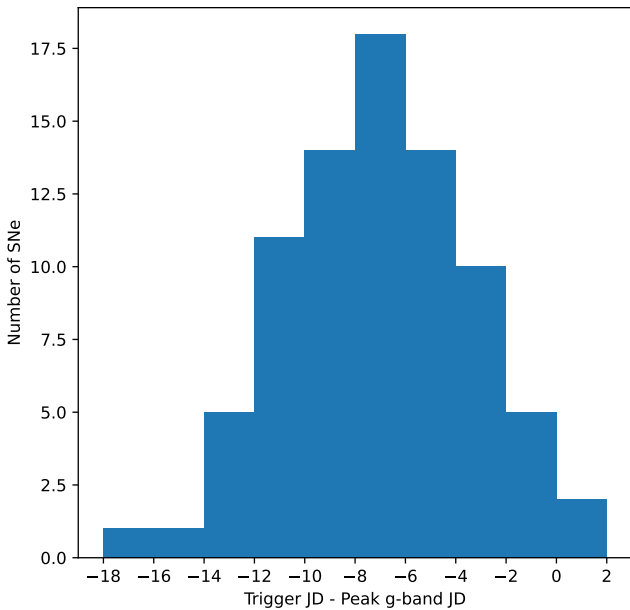
With the criteria adapted for use with LSST, we then investigated if our YSN selection criteria can increase the number of YSNs that TiDES could schedule for follow-up, thus increasing the number of early-time SN spectra in the TiDES SN sample. As LSST is not currently operational, we made use of the LSST simulation used by CF. This simulation utilises the LSST baseline V3.4 simulation<sup>3</sup> and the *SuperNova ANALysis* software (SNANA; Kessler et al. 2009) to produce a catalogue of SN events and photometry as would be observed by LSST. The transients included in this simulation are

<sup>3</sup> <https://survey-strategy.lsst.io/index.html> (accessed on 05/12/2024)

**Table 5.** Selection criteria that were applied to the LSST simulations of transient events to select YSNe. Provided are the criteria along with a description of their purpose.

\* This criterion is not applied to the LSST simulations but will be applied to LSST live alerts in the future.

Criterion	Reasoning
$g$ -, $i$ -, $r$ -, or $z$ -band magnitude $< 22.5$ mag $-70^\circ < \text{Declination} < 5^\circ$ Galactic latitude $< -10^\circ$ OR Galactic latitude $> 10^\circ$	Ensures that the object will meet the TiDES SN SSC Extent of 4MOST declination range Removal of Galactic transient sources
Number of $g$ -, $r$ -, $i$ -, or $z$ -band $> 5\sigma$ positive difference detections $\geq 2$ Sherlock classification not: VS, AGN, CV, BS *	Two or more $> 5\sigma$ detections in a band required for brightening rate criterion Removal of contaminants
Age $< 14$ days Brightening rate $> 0.2$ mag/day	Removes older objects that are unlikely pre-peak SNe Removes dimming and slow brightening sources that are unlikely to be YSNe.

**Figure 4.** Phase distribution of the TNS classified SNe in the YSN sample that was produced by applying our YSN selection criteria (see Table 1, and Sections 2.3.1 and 2.3.2) to 71 nights of ZTF live transient alerts.

SNe Ia, SNe Iax, SNe 91bg, SNe Ib, SNe Ic, SNe Ic-BL, SNe II, SNe IIb, SNe IIc, superluminous SNe (SLSNe), calcium rich transients (CART), and TDE. The simulations only include the LSST WFD and DDF surveys. The WFD survey covers a  $18000 \text{ deg}^2$  area that can be covered every 3 days by two of the *ugrizY* filter bands down to a depth of 25 mag in the *g*-band (Ivezić & LSST Science Collaboration 2018). The DDF survey is a much smaller area survey consisting of five circular fields<sup>4</sup> of diameter  $\sim 3.5^\circ$  that will have a higher cadence and a deeper coverage than that of the WFD survey (Ivezić & LSST Science Collaboration 2018).

## 3.2 LSST YSN Samples

### 3.2.1 LSST WFD Survey

Following the methods in Section 3.1, presented in Table 6 are the resulting samples of selected transients covering 5 years of the LSST WFD survey. This shows the total number of objects simulated, the number of objects selected by our YSN selection criteria (YSN sample), and the number of objects selected by the current TiDES selection criteria used by CF, hereafter referred to as the CF selection criteria and CF sample. We have also defined whether the objects were at a pre- or post-peak phase at the time of selection. The phase of selection was calculated using the peak date provided in the LSST simulation. As can be seen from Table 6, our YSN selection criteria selected 67388 transients, of which 48863 are SNe Ia. The YSN sample size is approximately only 9 percent of the size of the current simulated CF sample, and contains approximately 1.4 percent of the total number of simulated WFD survey transients.

For each classification of transient within our sample, we present in Figures 5–8 and Appendix A comparisons between the trigger (selection) phases for the samples produced by our selection criteria and the CF selection criteria. In general, the peak of the trigger distributions produced from our selection criteria occur a few days before those produced by the CF selection criteria. For example, Figure 5 shows that the SN Ia trigger phase distribution produced by our YSN criteria peaks at  $\sim -14$  days while the distribution produced by the CF peaks at  $\sim -6$  days. Furthermore, the two sided Kolmogorov–Smirnov (KS) tests performed on the YSN and CF phase distributions for each transient class all return P-values of 0.000, indicating that the two SN samples are drawn from different distributions.

For the majority of the transient classes, the trigger phase distributions produced by our selection criteria are unimodal. However, for SNe Ib (Figure 6) and SNe IIb (Figure 8) their trigger phase distributions display bimodality with the stronger of the peaks occurring  $\sim 25$  and  $\sim 15$  days after the weaker peaks respectively. The weaker of the peaks occur at a phase of  $\sim -40$  days for SNe Ib and  $\sim -15$  days for SNe IIb. The cause of the bimodality in the SN IIb trigger phase distribution is unclear. However, for the SN Ib distribution it arises due to the inclusion of SN 2005bf in the spectrophotometric templates used to simulate the transients in the LSST simulation. SN 2005bf is a transitional SN (Ib to Ic) and has a unique morphology, exhibiting two maxima separated by about 25 days and an unusually long rise to peak brightness of  $\sim 40$  days (Folatelli et al. 2006).

Lastly, the trigger phase distributions produced by our selection

<sup>4</sup> information of the 5th field: <https://community.lsst.org/t/scoc-endorsement-of-euclid-deep-field-south-observations/6406> (accessed on 25/09/2024)



**Table 6.** Resulting number of transients selected from the 5 year LSST WFD survey simulation by our YSN selection criteria (stated in Table 5) and the CF selection criteria. Additionally, provided (in brackets) is the percentage of transients that were selected from the total number of LSST WFD survey simulated transients.

5 Year WFD Survey					
Classification	Total Simulated	YSN Sample		CF Sample	
		Pre-Peak	Post-Peak	Pre-Peak	Post-Peak
Ia	2971223	48862 (1.64%)	1 (0.00%)	316269 (10.64%)	199698 (6.72%)
Iax	83351	738 (0.89%)	1 (0.00%)	5815 (7.00%)	5105 (6.12%)
91bg	69266	3082 (4.45%)	19 (0.03%)	9664 (13.95%)	10956 (15.82%)
Ib	89365	788 (0.88%)	0 (0.00%)	8095 (9.06%)	7303 (8.17%)
Ic	53670	794 (1.48%)	2 (0.00%)	3734 (6.96%)	5379 (10.02%)
Ic-BL	34511	392 (1.14%)	51 (0.15%)	1968 (5.70%)	3896 (11.29%)
II	782637	2942 (0.38%)	871 (0.11%)	4741 (0.61%)	74885 (9.57%)
IIb	220409	4176 (1.89%)	984 (0.45%)	13594 (6.17%)	28744 (13.04%)
IIc	483957	2709 (0.56%)	259 (0.05%)	11728 (2.42%)	33555 (6.93%)
SLSN	32922	352 (1.07%)	0 (0.00%)	9709 (29.49%)	8600 (26.12%)
CART	16719	161 (0.96%)	15 (0.09%)	589 (3.52%)	1640 (9.81%)
TDE	23476	189 (0.81%)	0 (0.00%)	2261 (9.63%)	1523 (6.49%)
Total	4861506	65185 (1.34%)	2203 (0.05%)	388167 (7.98%)	381284 (7.84%)

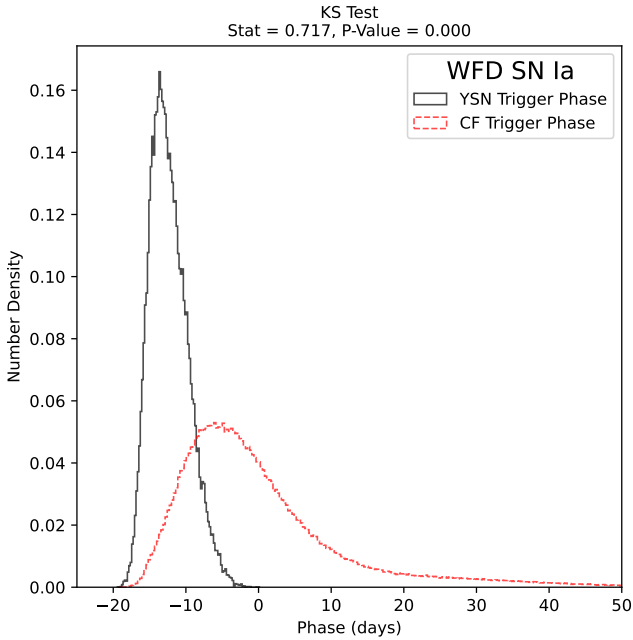


**Figure 5.** Comparison between the SN Ia trigger phase distributions produced by applying our selection criteria (YSN; see Table 5) and the CF selection criteria to the LSST WFD survey simulation. Note that phase has been truncated at 50 days.

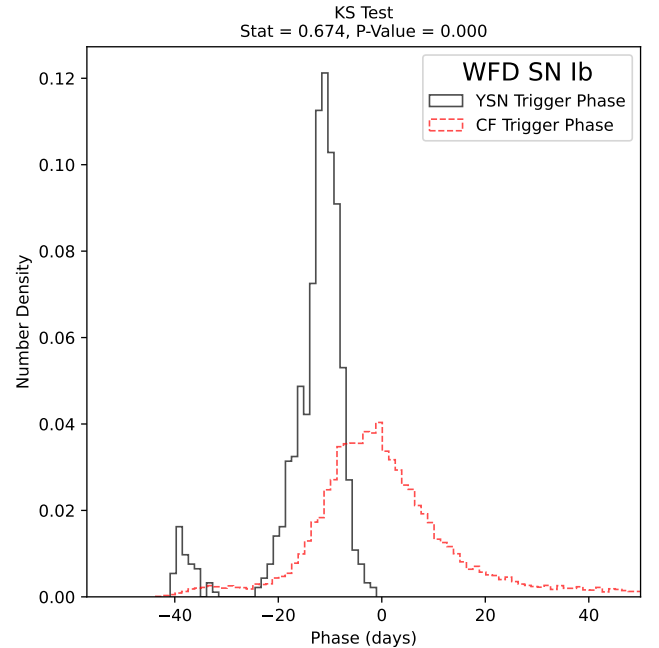


**Figure 6.** Comparison between the SN Ib trigger phase distributions produced by applying our selection criteria (YSN; see Table 5) and the CF selection criteria to the LSST WFD survey simulation. Note that phase has been truncated at 50 days.

criteria for many of the transient classes do not exceed into positive phases (post-peak), as is seen in Figures 5, 6, and 7. However, for SNe II, IIb, IIc, and Ic-BL (see Figure 8) the trigger phase distributions extend up to phases of 10 days.

To gain a better understanding of the crossover between the objects selected by our YSN criteria and the CF criteria, we present in Table 7 the number of selected transients that are common to both sets of selection criteria. We also include the number of transients that are only selected by our selection criteria. As is seen, there are 47722

SNe Ia and 17369 non-SNe Ia that are commonly selected by both sets of selection criteria. Also indicated is that our selection criteria selects an additional 1141 SNe Ia and 1137 non-SNe Ia that the CF selection criteria does not select.

Additionally, for each of the commonly selected LSST WFD survey transients, we compared the difference between their trigger phases when selected by our YSN selection criteria and the CF criteria. Presented in Figure 9 is the distribution of the trigger differences. As is shown, the majority of transients (~40000) have a negative time

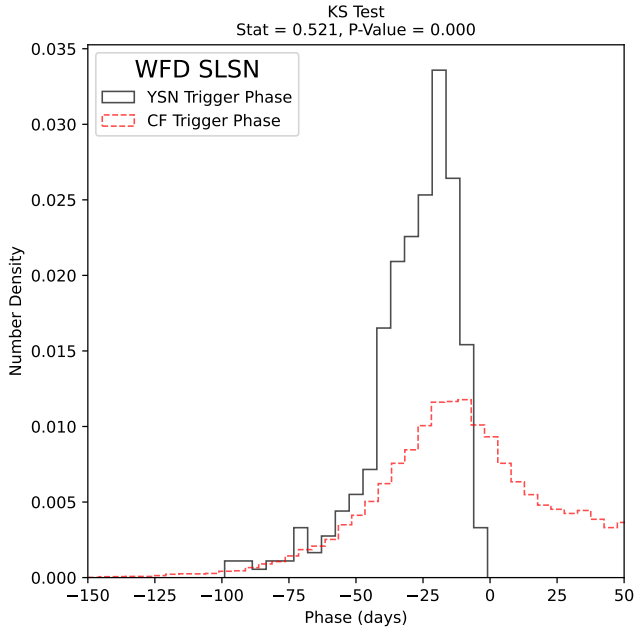


**Figure 7.** Comparison between the SLSN trigger phase distributions produced by applying our selection criteria (YSN; see Table 5) and the CF selection criteria to the LSST WFD survey simulation. Note that phase has been truncated at -150 and 50 days.

**Table 7.** Number of LSST WFD simulated transients that were commonly selected by both our YSN selection criteria (see Table 5) and the CF selection criteria. Also included is the number of simulated transients that were only selected by our YSN criteria. Additionally, provided (in brackets) is the number of commonly (YSN uniquely) selected simulated transients as percentage of the total number of commonly (YSN uniquely) selected transients.

Classification	Commonly Selected	YSN Uniquely Selected
Ia	47722 (78.76%)	1141 (50.09%)
Iax	725 (1.20%)	14 (0.61%)
91bg	2953 (4.87%)	129 (5.66%)
Ib	771 (1.27%)	17 (0.75%)
Ic	776 (1.28%)	20 (0.88%)
Ic-BL	430 (0.71%)	13 (0.57%)
II	3737 (6.17%)	76 (3.34%)
I Ib	4380 (7.23%)	780 (34.24%)
I In	2889 (4.77%)	79 (3.47%)
SLSN	350 (0.58%)	2 (0.09%)
CART	172 (0.28%)	4 (0.18%)
TDE	186 (0.31%)	3 (0.13%)
Total	60591	2278

difference, or in other words were selected by the YSN selection criteria before the CF selection criteria, with some transients selected more than 100 days earlier. Meanwhile, approximately 25000 of the commonly selected transients are selected up to 12 days earlier by the CF selection criteria compared to our YSN criteria.

### 3.2.2 LSST DDF Survey

Following the methods presented in Section 3.1, presented in Table 8 are the resulting YSN and CF samples of selected transients from the

5 year LSST DDF survey. As is shown, our YSN selection criteria selects 1167 transients, of which only 38 were selected at post-peak phases. In contrast, the CF sample contains 7757 transients, of which 2922 were selected after peak brightness.

To investigate if our selection criteria selects YSNe, we present in Figures 10, 11, and 12 the trigger phase distributions for SNe Ia, 91bg, and I Ib that were produced by our selection criteria and the CF criteria. We present in Appendix B the phase distributions for the other classes of transients. However, it should be noted that the classes presented in Appendix B suffer from low number statistics and are only included for completeness.

Figures 10 and 11 show that for SNe Ia and 91bg-like SNe (a subset of SNe Ia) the trigger distributions produced by our selection criteria are unimodal with peaks that occur approximately 5 days before those produced by the CF selection criteria. Furthermore, our selection criteria is shown to only select pre-peak SNe Ia, with a maximum trigger phase of approximately -5 days. The two-sided KS tests performed on the distributions for both the SNe Ia and 91bg both returned P-values of 0.000, indicating that the trigger phase distributions of the YSN and CF samples are drawn from different distributions.

In contrast, the SNe I Ib trigger phase distributions, presented in Figure 12, show that our selection criteria produces a trigger phase distribution that is bimodal, with the dominant peak occurring at a phase of  $\sim -1$  day, which is approximately the same as the trigger phase distribution produced by the CF selection criteria. The secondary peak of the distribution occurs at a phase of  $\sim -15$  days. As with the WFD SNe I Ib, the cause of this bimodality unclear. The distribution displayed in Figure 12 also shows that our selection criteria selects some (20 from Table 8) post-peak SNe I Ib, with a maximum trigger phase of  $\sim 4$  days.

As with the LSST WFD survey samples, to understand the crossover between the objects selected by our YSN selection criteria and the CF selection criteria, we present in Table 9 the number of selected transients that are common to both sets of selection criteria. We also include the number of transients that are only selected by our selection criteria. As is shown, there are 866 SNe Ia and 291 non-SNe Ia that are commonly selected. Our YSN selection criteria selects only 9 transients that were not selected by the CF selection criteria.

For the commonly selected LSST DDF survey transients, we directly compared the times at which they were triggered on by the two sets of selection criteria. Presented in Figure 13 is the distribution of the time difference between when a commonly selected target was selected by our YSN selection criteria and the CF selection criteria. As indicated, approximately 900 of the commonly selected transients have a positive time difference (selected by the CF criteria first) up to a maximum of 6 days. The remaining  $\sim 250$  commonly selected transients are shown to have a negative time difference (selected by YSN criteria first) as low as -18 days, with the exception of one transient with a time difference of -96 days.

## 3.3 YSN Selection Criteria Performance on LSST Simulations

### 3.3.1 SN Sample Size

From our results, presented in Section 3.2, it is evident from Tables 6 and 8 that our selection criteria produces a sample of transients that is not insignificant in number. From the 5 year LSST simulation, our YSN criteria selected a total of 67388 WFD survey transients and 1167 DDF survey transients for follow-up observations. However, our YSN samples are much smaller than the samples produced by the

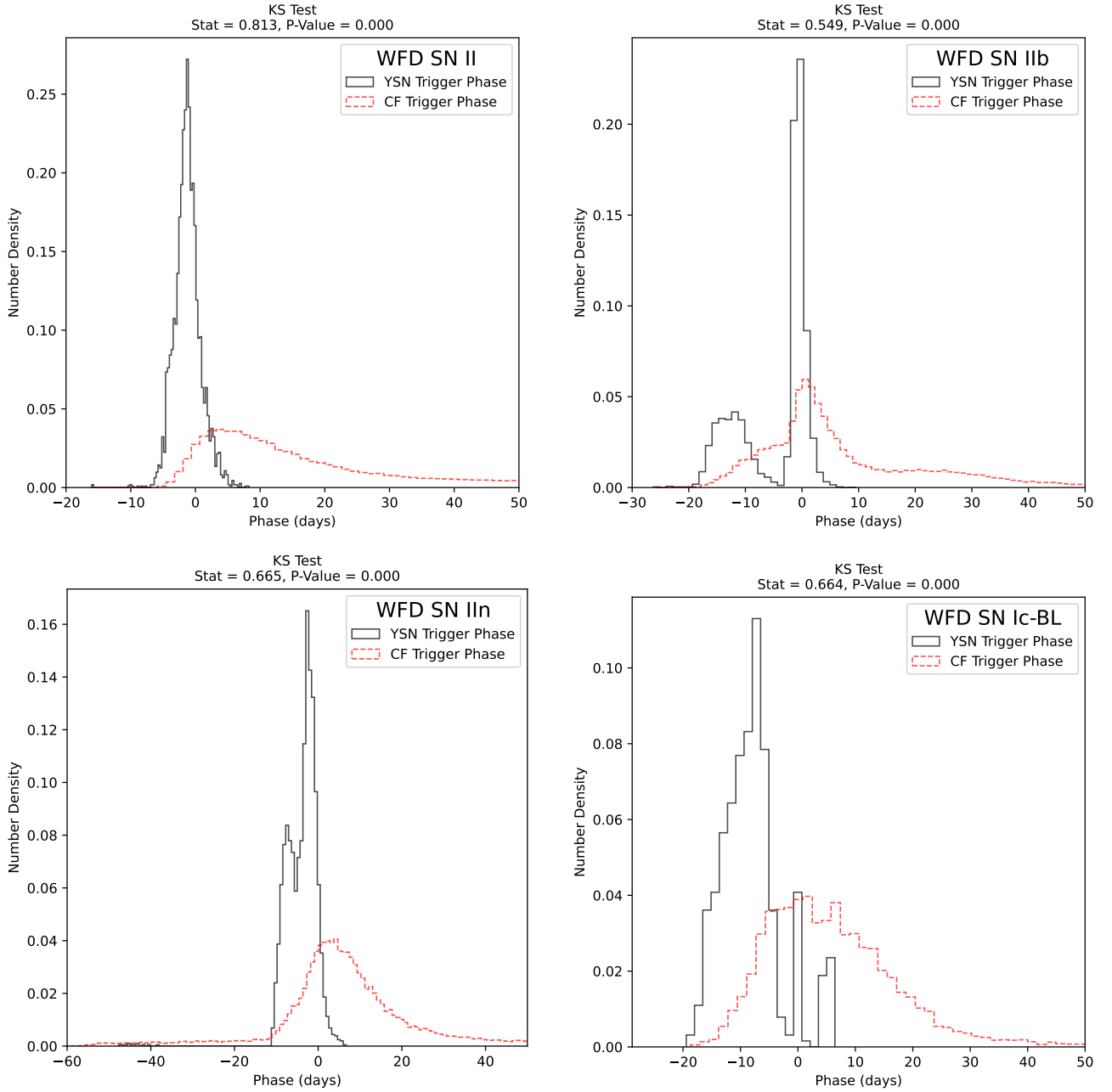


**Figure 8.** Comparison between the SN II, IIb, IIc and Ic-BL trigger phase distributions produced by applying our selection criteria (YSN; see Table 5) and the CF selection criteria to the LSST WFD survey simulation. Note that all phases have been truncated at 50 days.

CF selection criteria, with their WFD and DDF samples containing  $\sim 11$  and  $\sim 7$  times more transients respectively. Although our YSN sample of selected transients is smaller than the CF sample, the aim of our selection criteria is not to replace the current TiDES selection criteria (CF criteria). Instead our YSN selection criteria are to be used in conjunction with the CF criteria, with the aim of selecting some of the transients at earlier phases. With this in mind, the size of our YSN sample indicates that incorporating our selection criteria into the TiDES survey has the potential to have a non-insignificant affect on the resulting SN sample.

### 3.3.2 SN Early Selection Effectiveness

Our selection criteria were developed for selecting SNe at earlier phases than the current TiDES selection criteria (CF criteria) to enhance the TiDES YSN sample. Our results presented in Section 3.2, specifically Figures 5-8 and 10-12, showed that our selection criteria can select SN at earlier phases than the CF selection criteria. From Figure 5, it is shown that for the LSST WFD SNe Ia the trigger phase distribution produced by our selection criteria peaks approximately 10 days before the trigger phase distribution produced by the CF selection criteria. This general trend is seen for all of the transient classes across both the WFD and DDF surveys (where there is no low number statistics), which indicates that our selection criteria on aver-

**Table 8.** Resulting number of transients selected from the 5 year LSST DDF survey simulation by our YSN selection criteria (stated in Table 5) and the CF selection criteria. Additionally, provided (in brackets) is the percentage of transients that were selected from the total number of LSST DDF survey simulated transients.

5 Year DDF Survey					
Classification	Total Simulated	YSN Sample		CF sample	
		Pre-Peak	Post-Peak	Pre-Peak	Post-Peak
Ia	57504	869 (1.51%)	0 (0.00%)	3956 (6.88%)	1352 (2.35%)
Iax	2384	9 (0.38%)	0 (0.00%)	63 (2.64%)	48 (2.01%)
91bg	1532	55 (3.59%)	1 (0.07%)	142 (9.27%)	84 (5.48%)
Ib	2558	8 (0.31%)	0 (0.00%)	96 (3.75%)	43 (1.68%)
Ic	1665	12 (0.72%)	0 (0.00%)	44 (2.64%)	55 (3.30%)
Ic-BL	797	9 (1.13%)	1 (0.13%)	26 (3.26%)	26 (3.26%)
II	27260	47 (0.17%)	11 (0.04%)	81 (0.30%)	667 (2.45%)
IIb	5057	59 (1.17%)	20 (0.40%)	176 (3.48%)	285 (5.64%)
IIin	9853	52 (0.53%)	4 (0.04%)	156 (1.58%)	279 (2.83%)
SLSN	228	4 (1.75%)	0 (0.00%)	74 (32.46%)	58 (25.44%)
CART	583	1 (0.17%)	1 (0.17%)	2 (0.34%)	13 (2.23%)
TDE	293	4 (1.37%)	0 (0.00%)	19 (6.48%)	12 (4.10%)
Total	109714	1129 (1.03%)	38 (0.03%)	4835 (4.41%)	2922 (2.66%)

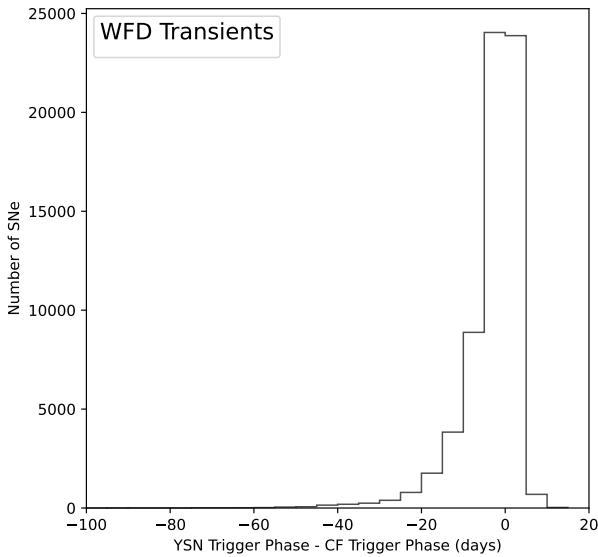


**Figure 9.** Distribution of the time differences of the selection of the LSST WFD transients that were selected by both our YSN selection criteria and the CF criteria. Note that all of the simulated transient types (see Table 6) are included.

age selects younger objects than the CF criteria, therefore enhancing the early SN sample in the TiDES transient programme.

However, there are two transient classes, SLSN and SN IIin, where the CF selection criteria can select the SN at earlier phases than our YSN criteria. While the phase distributions for these SN classes produced by our selection criteria have a peak at earlier phases, the CF criteria is able to select SLSN and SN IIin over 50 days earlier than our YSN criteria. This is demonstrated in Figures 7 and 8 (bottom left). For example, for the WFD survey SLSNe, the CF selection criteria was able to select them as early as ~200 days before peak while our

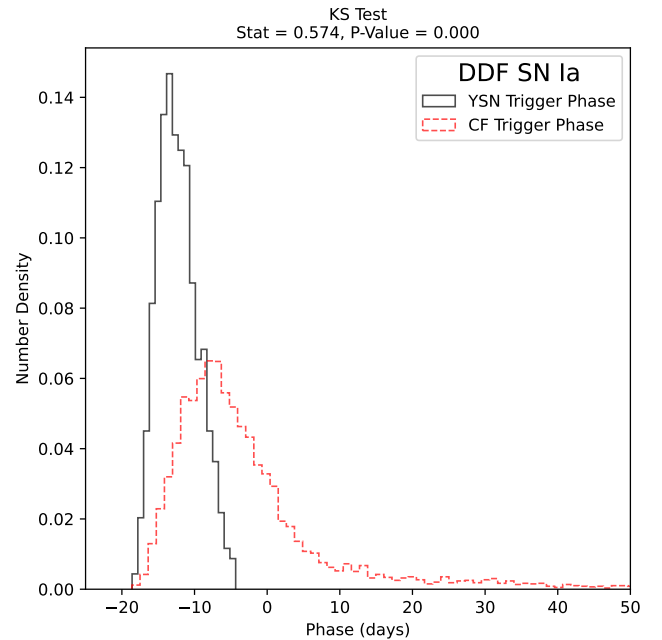


**Figure 10.** Comparison between the SN Ia trigger phase distributions produced by applying our selection criteria (YSN; see Table 5) and the CF selection criteria to the LSST DDF survey simulation. Note that phase has been truncated at 50 days.

YSN selection criteria only selected them as early as ~100 days before peak. However, these early detections are unrealistic, likely resulting from the over-extrapolation of the spectrophotometric templates used in the simulation of their LSST photometry. Although an artefact of the simulations, the earlier triggering by the CF criteria highlights that our selection criteria may not be optimised for each transient class. Specifically, transient types that exhibit an initial relatively slow phase of brightening in their early evolution, such as SLSNe, will not be selected at these early phases by our YSN selection

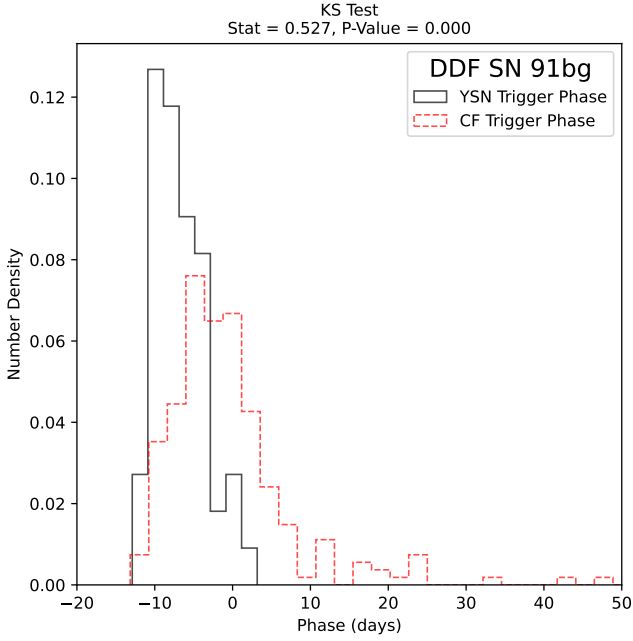


**Figure 11.** Comparison between the SN 91bg trigger phase distributions produced by applying our selection criteria (YSN; see Table 5) and the CF selection criteria to the LSST DDF survey simulation. Note that phase has been truncated at 50 days.

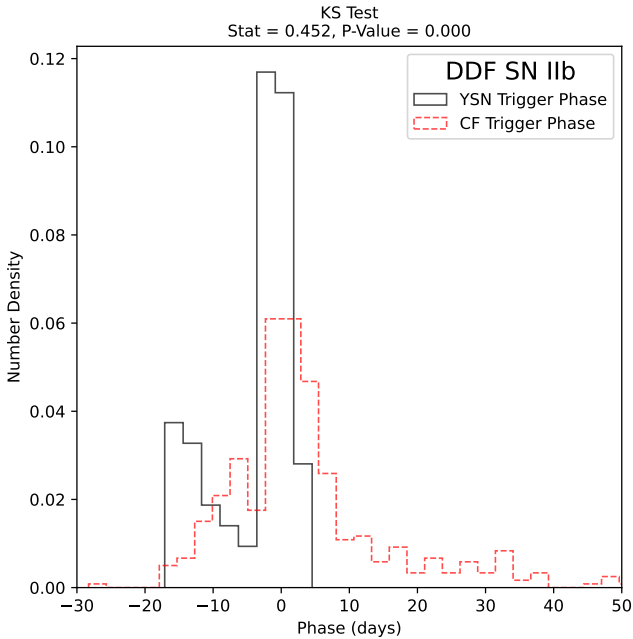


**Figure 12.** Comparison between the SN IIb trigger phase distributions produced by applying our selection criteria (YSN; see Table 5) and the CF selection criteria to the LSST DDF survey simulation. Note that phase has been truncated at 50 days.

**Table 9.** Number of LSST DDF simulated transients that were commonly selected by both our YSN selection criteria (see Table 5) and the CF criteria. Also included is the number of simulated transients that were only selected by our YSN criteria. Additionally, provided (in brackets) is the number of commonly (YSN uniquely) selected simulated transients as percentage of the total number of commonly (YSN uniquely) selected transients.

Classification	Commonly Selected	YSN Uniquely Selected
Ia	866 (74.85%)	3 (33.33%)
Iax	9 (0.78%)	0 (0.00%)
91bg	55 (4.75%)	0 (0.00%)
Ib	8 (0.69%)	0 (0.00%)
Ic	11 (0.95%)	1 (11.11%)
Ic-BL	9 (0.78%)	1 (11.11%)
II	57 (4.93%)	1 (11.11%)
IIb	77 (6.66%)	2 (22.22%)
IIc	55 (4.75%)	1 (11.11%)
SLSN	4 (0.35%)	0 (0.00%)
CART	2 (0.17%)	0 (0.00%)
TDE	4 (0.35%)	0 (0.00%)
Total	1157	9

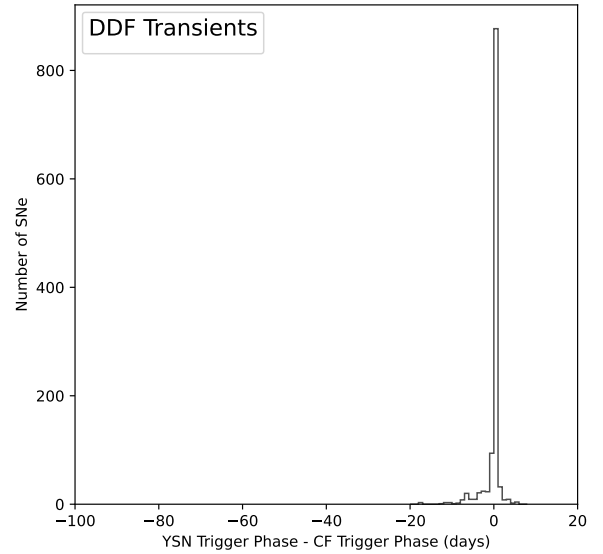


**Figure 13.** Distribution of the time differences of the selection of the LSST DDF transients that were selected by both our YSN selection criteria and the CF criteria. Note that all of the simulated transient types (see Table 6) are included.

criteria due to the brightening rate criterion, which is designed to reject slowly brightening sources.

To gain a better understanding of how our YSN selection criteria performed, we compared the transients that were commonly selected by both the YSN and CF selection criteria. As shown by Figures 9 and 13, our YSN selection criteria was able to select ~40000 WFD survey transients and ~250 DDF survey transients at earlier times than the CF criteria. While many of these transients were selected up to 50 days earlier, some were selected up to 300 days earlier. This demonstrates that our YSN selection criteria can prove very useful

for selecting transients at phases earlier than is currently possible with the CF criteria.

On the contrary, the CF selection criteria triggered on  $\sim 25000$  WFD and  $\sim 900$  DDF survey transients earlier than our YSN selection criteria. However, upon further investigation, many of these transients ( $\sim 20000$ ) were selected within the same night but from observations taken at different times. Considering that TiDES will not be able to follow-up a selected transient within the same night, due to there being no target of opportunity mode on 4MOST, a few hours difference between the YSN and CF selection criteria triggers will have no effect on when the selected SN could potentially be followed-up by TiDES. Investigating the remaining  $\sim 5000$  transients, it was found that the CF criteria triggered on many of them before our YSN criteria because they lacked multiple observations in same filter. At least two observations in a filter are required to calculate the brightening rate used in the YSN selection criteria, whereas the CF criteria does not require multiple observations in one filter and so can select some targets earlier than our YSN criteria. To solve this issue the brightening rate criterion would have to be removed from our selection criteria. However, as demonstrated in Section 2.3.2, the brightening rate criterion is used to limit the contamination (non-SNe sources and post-peak SNe) that is selected. Therefore, with this in mind and considering the improvements in earlier triggering of  $\sim 40000$  SNe, we believe that our YSN selection criteria is suitable to be implemented in to the TiDES survey. However, we must finally consider the potential contamination of the YSN sample in order to determine if we should implement our YSN selection criteria into the TiDES survey.

### 3.3.3 SN Sample Contamination

As previously discussed in Section 2.3.3, our YSN selection criteria should have a sufficiently high purity (low contamination). From our ZTF YSN sample, we calculated that the contamination of the ZTF YSN sample was  $\sim 28$  percent, however, we could not conclude if this level of contamination was sufficiently low to not waste too many of TiDES's fibre hours. By extrapolating the level of contamination from the ZTF YSN sample to the LSST YSN sample, we can estimate how many fibre hours TiDES will potentially waste on non-SN sources. From Tables 6 and 8, it is shown that the selected YSN sample (WFD and DDF samples combined) contains 66121 pre-peak selected SNe (exclusion of TDE), 2241 post-peak selected SNe, and 193 TDE. Assuming that the contamination of the ZTF and LSST samples will be comparable, the number of contaminants (non pre-peak selected SNe) that would be selected as part of the LSST YSN sample is 25714 objects ( $66121 \times 0.28 / (1 - 0.28)$ ).

To estimate how many of these could be observed by 4MOST, we begin by making a few assumptions: 4MOST observes for on average 9 hours per night (Guiglion et al. 2019), an average 4MOST pointing lasts 1 hour, and 15 SNe are observed per 4MOST pointing. Based on these assumptions, 4MOST can observe an estimated 135 SNe per night. 4MOST is a 5 year long survey, however, approximately 300 nights per year at Paranal are usable for observations (Guiglion et al. 2019), resulting in an estimated 1500 observable nights over the lifetime of 4MOST. As a result, an optimistic estimate suggests that 4MOST could observe up to 202,500 SNe over its lifetime. This is much less than the total number of unique transients that are selected by our criteria and the CF criteria for follow-up with 4MOST, which is approximately 780,000 transients. Therefore, up to approximately 26 percent of the selected samples can be estimated to be observed by 4MOST, which means that about 6676 ( $25714 \times 0.26$ ) contaminants are observed over the lifetime of TiDES.

In the case of the TiDES survey, post-peak SNe are not considered contaminants and so we need to remove the observed post-peak selected SNe from the previously calculated number of observed contaminants (6676). There are 2241 post-peak selected SNe in our YSN sample, of which about 582 ( $2241 \times 0.26$ ) can be assumed to be observed. Therefore, an estimated 6094 ( $6676 - 582$ ) non-SN objects are observed over the life span of TiDES by using our YSN selection criteria.

By assuming that each observed object receives 40 minutes of observation time, over the lifetime of TiDES (5 years) the fibre hours (observing time) wasted on the non-SN objects is  $\sim 4063$  hours ( $40 \text{ mins} \times 6094$ ). This is equates to approximately 1.6 percent of TiDES's total available fibre hours (250000 hours (CF)) or 4.1 percent of the fibre hours allocated for the TiDES SN survey (100000 fibre hours, 40 percent of the entirety of TiDES). Based on these estimates, we consider our selection criteria capable of producing a pure enough sample as to not waste too many fibre hours on non-SNe targets.

## 4 OPTIMAL 4MOST STRATEGY

The TiDES survey will spectroscopically follow-up transients that are selected from the LSST live transient alerts using 4MOST. As of now, there is no coordination between the observing strategies of LSST and 4MOST, which results in an unknown variable delay between the triggering of an LSST SN and its follow-up 4MOST observation. This leads to many cases where the signal to noise ratio (SNR) of a 4MOST observed SN spectrum is much lower than its highest obtainable SNR. Furthermore, the lack of coordination also negatively impacts our YSN selection criteria, as the unknown variable delay could be days, weeks, or even months, at which point a selected YSN has evolved and is likely no longer an early-time SN. To fully utilise our YSN selection criteria 4MOST would have to follow-up the targets within a few days of selection. Therefore, we propose to construct a 4MOST observing strategy for the case of maximising transient follow-up.

To optimise the 4MOST observing strategy for the case of TiDES and our YSN selection criteria, we propose that the 4MOST strategy follows (with some delay) the LSST observing strategy. In theory, this strategy would result in our LSST selected targets always being observed by 4MOST soon after their selection. This should increase the number of observed targets, improve the SN spectra SNR, and aid in obtaining early-time SN spectra. There are of course caveats to consider regarding the feasibility of 4MOST following the strategy of LSST. For example, LSST will observe the southern sky approximately every 3 days<sup>5</sup>, which is not possible with 4MOST, resulting in some LSST fields having to be skipped by 4MOST. As such, in this work we do not seek to construct a full 4MOST observing strategy, but instead we investigate and suggest guidelines for future works towards designing and simulating a full 4MOST observing strategy for time-domain science. Furthermore, we only investigate 4MOST strategies that cover the LSST WFD fields, as 4MOST will implement a cadence based observing strategy for the fields in the DDF survey based on requirements from the TiDES reverberation mapping survey (CF) and other 4MOST surveys.

<sup>5</sup> <https://survey-strategy.lsst.io/baseline/wfd.html>

## 4.1 Investigating Observing Strategies

### 4.1.1 Simulating 4MOST SN Spectra

To simulate a SN spectrum as observed by 4MOST, for a given SN in the LSST simulation that was used in Section 3, we first created its template spectrum at a given phase. This was achieved by using the Python package SNeCosmo (Barbary et al. 2024), which can extract a template spectrum from a spectrophotometric model for the given input parameters. Different models have different input parameters, for example SN Ia simulated with the extended SALT2 model (Hounsell et al. 2018) require the parameters of redshift, phase, SALT2 colour parameter, SALT2 stretch parameter, and apparent magnitude. Whereas a SN II simulated using the models of Vincenzi et al. (2019) requires only phase, redshift, and apparent magnitude. The spectrophotometric model and its input parameters for each of the SN in the LSST simulation are recorded in the simulation output files.

To the template spectra, we also applied the effect of Galactic extinction, which was achieved by using the SNeCosmo method “F99Dust” that applies the extinction model of Fitzpatrick (1999). We used the total-to-selective extinction ratio  $R_V = 3.1$  and the extinction values defined for each SN in the LSST simulation output files. Although we included Galactic contamination in our SN spectral templates, we did not attempt to include contamination from the SNe’s host galaxy.

With the template spectra created, we then simulated the effects of observing the SN spectra with 4MOST, which was accomplished by using the 4MOST exposure time calculator (ETC)<sup>6</sup>. As we simulated observed spectra for TiDES, we used the low-resolution spectrograph as this will be used by TiDES during operations (CF). For the observing conditions, we assumed the following typical observing conditions for TiDES targets: zenith angle of 45 deg, seeing of 0.8 arcsec, grey sky brightness, and an exposure time of 40 minutes. Although having constant observing conditions for all targets is unrealistic, varying the observing conditions would require development of a full 4MOST observing strategy, which is outside the scope of this work.

### 4.1.2 Applying an Observing Strategy

As previously mentioned, we investigated 4MOST WFD observing strategies that follow LSST with a delay time. To accomplish this, we applied our methods presented in Section 4.1.1 to the CF and YSN WFD SN samples produced and presented in Section 3, simulating their 4MOST observed spectra. To apply the 4MOST observing strategies with different delay times, we altered the phases at which the template spectra were created for. The phase that was used to produce a given SN’s template spectrum is given as the phase at which the SN was triggered on plus the time delay of the 4MOST observing strategy. For example, a LSST SN selected at a phase of  $-10.5$  days would be observed by a 4MOST strategy with a 3 day time delay at a phase of  $-7.5$  days. Using these methods, we simulated the spectra for the LSST selected CF and YSN WFD samples as if they had been observed using 4MOST observing strategies with delay times of 1, 3, 5, and 7 days.

<sup>6</sup> We used the Python API of the 4MOST ETC (<https://science.aip.de/readthedocs/OpSys/etc/master/index.html>).

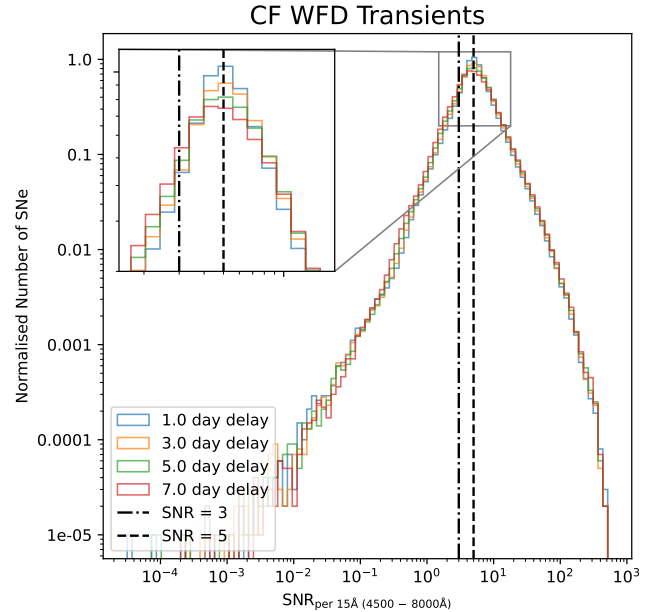


**Figure 14.** The CF LSST selected WFD SN sample’s observed spectral  $\text{SNR}_{15\text{\AA}}$  distributions. The SNe were observed using 4MOST observing strategies that followed the LSST strategy by 1, 3, 5, and 7 days.

### 4.1.3 Investigating Observing Strategy Effects

To investigate the effects that the different time delays of the 4MOST observing strategy have on the resulting spectroscopically observed SN sample, we inspected the SNR of the spectra. Specifically, we analysed the observed SN samples’ SNR distributions as well as the percentage of simulated SNe whose spectra exceeded certain SNR thresholds. Following CF we chose to define the SNR of a spectrum as the mean SNR in  $15\text{\AA}$  bins over the observer frame wavelengths  $4500 - 8000\text{\AA}$ , hereafter denoted as  $\text{SNR}_{15\text{\AA}}$ .  $\text{SNR}_{15\text{\AA}}$  thresholds of 5 and 3 were chosen as they can be used as a proxy for how reliably a SN spectrum can be classified. Balland et al. (2009) showed that spectra with a  $\text{SNR}_{15\text{\AA}} > 5$  provides reliable classifications, while a possible classification was achievable for spectra with a  $\text{SNR}_{15\text{\AA}}$  as low as 3. For the purpose of our study, using the SNR as a proxy for the reliability of the SN classifications is satisfactory. However, for a more in depth analysis of the SN classification reliability of 4MOST-like spectra, we refer the reader to Milligan & Hook, (in prep.). Although the chosen SNR thresholds are a good proxy for spectra classifications, we also kept in mind that we want to maximise the spectra’s SNR in order to reliably extract the spectral information required for performing astrophysical studies of SN.

## 4.2 4MOST Observed SN Samples

### 4.2.1 CF Sample

Following the methods of Section 4.1, we present in Figure 14 the SNR distributions of the observed CF WFD SN sample’s spectra following observations with the 4MOST strategies that follow the strategy of LSST with a 1, 3, 5, or 7 day delay. As is shown, the different observing strategies all produce similar SNR distributions that have no significantly notable differences. The SNR distributions of the 4MOST observed spectra all peak at a  $\text{SNR}_{15\text{\AA}}$  of 5 regardless of the 4MOST observing strategy.

**Table 10.** For both the LSST selected WFD SN samples (CF WFD and YSN WFD), presented are the percentages of 4MOST observed SNe whose spectra exceeded a  $\text{SNR}_{15\text{\AA}}$  of 5 or a  $\text{SNR}_{15\text{\AA}}$  of 3. These results are provided for the 4MOST observing strategies that follow the LSST strategy by delays of 1, 3, 5, and 7 days.

4MOST Observing Strategies	SN Sample			
	CF WFD		YSN WFD	
	SNR > 3	SNR > 5	SNR > 3	SNR > 5
1 Day Delay	81.2%	50.8%	94.7%	77.4%
3 Day Delay	79.7%	51.5%	95.6%	87.0%
5 Day Delay	77.8%	50.1%	95.5%	88.7%
7 Day Delay	75.2%	47.7%	95.0%	88.9%

In addition to the  $\text{SNR}_{15\text{\AA}}$  distributions, we present in Table 10 the percentage of transients whose observed 4MOST spectra exceed a  $\text{SNR}_{15\text{\AA}}$  of 5 or 3 when observed using the 4MOST observing strategies that follow the LSST strategy with a 1, 3, 5, and 7 day delay. From the table it is shown that of the SNe observed under any of the investigated 4MOST observing strategies, more than 47.7 percent (75.2 percent) of the observed CF WFD SNe have a  $\text{SNR}_{15\text{\AA}} > 5 (> 3)$ . Table 10 also demonstrates that as the time delay between the LSST and 4MOST observing strategies increases, the percentage of observed CF WFD SNe with a  $\text{SNR}_{15\text{\AA}} > 3$  decreases. This trend is not seen for the percentage of observed CF WFD SNe with a  $\text{SNR}_{15\text{\AA}} > 5$ , as the maximum percentage occurs with the 3 day delayed 4MOST observing strategy. The percentage of observed CF WFD SNe with a  $\text{SNR}_{15\text{\AA}} > 5$  under the 3 day delayed strategy is 51.5 percent, while the strategies with a 1, 3, and 7 day delays all have percentages that are more than 0.7 percent less than the 3 day delay strategy.

#### 4.2.2 YSN Sample

As with the CF sample, we present in Figure 15 the SNR distributions of the observed YSN WFD SN sample's spectra following observations with the 4MOST strategies that follow the strategy of LSST with a 1, 3, 5, or 7 day delay. As is shown, the different observing strategies all produce similarly shaped SNR distributions. The peaks of the SNR distributions for the different observing strategies are shifted to higher SNR the larger the strategy's time delay is. For example, the YSN WFD sample observed using the 7 day delayed 4MOST strategy peaks at a  $\text{SNR}_{15\text{\AA}}$  of  $\sim 10$ , while the 1 day delayed strategy peaks at a  $\text{SNR}_{15\text{\AA}}$  of  $\sim 6$ .

In addition, we also present in Table 10, the percentage of transients whose observed 4MOST spectra exceed a  $\text{SNR}_{15\text{\AA}}$  of 5 or 3 when observed using the 4MOST observing strategies that follow the LSST strategy with a 1, 3, 5, and 7 day delay. As the Table shows, the percentage of observed YSN WFD SN spectra whose  $\text{SNR}_{15\text{\AA}}$  is greater than 5 increases as the delay between the 4MOST and LSST observing strategies is increased, with 88.9 percent of WFD YSN observed having a  $\text{SNR}_{15\text{\AA}} > 5$  under the 7 day delayed 4MOST strategy. In contrast, the percentage of observed WFD YSN whose spectra have a  $\text{SNR}_{15\text{\AA}} > 3$  is at maximum when the 4MOST 3 day delayed strategy is applied.

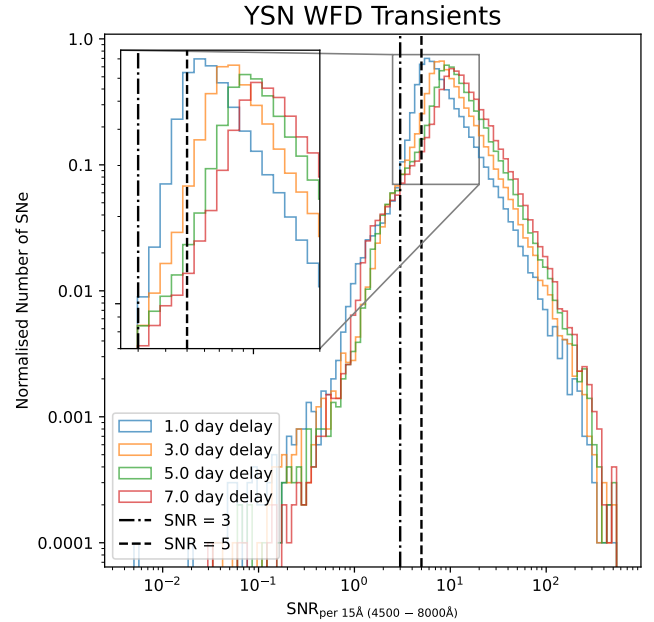


**Figure 15.** The YSN LSST selected WFD SN sample's observed spectral  $\text{SNR}_{15\text{\AA}}$  distributions. The SNe were observed using 4MOST observing strategies that followed the LSST strategy by 1, 3, 5, and 7 days.

### 4.3 Discussion

#### 4.3.1 CF Sample

The results presented in Section 4.2.1, showed that the percentage of observed CF WFD SN whose spectra have a  $\text{SNR}_{15\text{\AA}} > 3$  decreases as the observing strategy time delay is increased from 1 day to 7 days. This suggests that a time delay between the LSST and 4MOST observing of 1 day is the most optimal delay for obtaining the most spectra with a  $\text{SNR}_{15\text{\AA}} > 3$ . On the contrary, the highest percentage of observed SN with a spectra whose  $\text{SNR}_{15\text{\AA}}$  is  $> 5$  occurred when applying the 3 day delayed strategy, suggesting that this could be the more optimal strategy. However, we must also consider the significance of the  $\text{SNR}_{15\text{\AA}}$  thresholds of 5 and 3. As shown by Balland et al. (2009), SN spectra with a  $\text{SNR}_{15\text{\AA}} > 5$  can be reliably classified, while classifications from spectra with a  $\text{SNR}_{15\text{\AA}}$  as low as 3 are possible but less reliable.

Taking the significance of the SNR thresholds into consideration, using a 1 day delayed 4MOST observing strategy provides the highest percentage of observed SN that are likely to be classified, 81.2 percent of the CF WFD sample. This is 1.5 percent more than observed with the 3 day delayed strategy. However, the 3 day delayed 4MOST strategy provides the most spectra that could be reliably classified, 51.5 percent of the Frohamier WFD SN sample, which is 0.7 percent more than observed with the 1 day delayed strategy.

For the case of the CF SN sample, to determine which strategy is optimal depends on if one values the prospect of obtaining more SN classifications over the reliability of the classifications. The TiDES SN survey values the reliability of the classifications and the physics that can be constrained from the spectra. Therefore, a 3 day delayed 4MOST observing strategy, which provides the highest percentage of spectra that can reliably classified ( $\text{SNR}_{15\text{\AA}} > 5$ ), is more optimal for the CF SN sample.



### 4.3.2 YSN Sample

For TiDES to fully capitalise on the earlier SN triggers provided by our YSN selection criteria, quick follow up of the YSN targets is required. Ideally a triggered event would be followed up within minutes, however, this is not possible for the TiDES survey as 4MOST will not be used for targets of opportunity. As such, the earliest that 4MOST could feasibly provide an observation of a triggered target is within the following night after the trigger. Therefore, a 4MOST observing strategy that follows the LSST observing strategy with a delay of 1 day is most optimal for making the most out of our YSN selection criteria's early triggers. However, we must also consider the quality of the sample in terms of the classification reliability and overall SNR distribution.

The results presented in Section 4.2.2 showed that the SNR distribution (see Figure 15) is shifted to higher SNR as the delay time is increased. This was also demonstrated by Table 10, which showed that the percentage of observed SNe whose spectral SNR exceeded a  $\text{SNR}_{15\text{\AA}}$  of 5 was highest when the 7 day delayed 4MOST strategy was used. This result can be explained through the trigger phase distributions of our YSN targets (see Figures 5 - 8), which showed that the YSN targets are predominantly selected at pre-peak phases, with the majority selected before a phase of  $\sim -14$  days. As the 4MOST observing strategy time delay is increased, the number of SNe that evolve to near peak brightness increases, resulting in an increase in the number of SNe that are bright enough such that their spectral  $\text{SNR}_{15\text{\AA}} > 5$ . Based on our YSN trigger phase distributions showing that many of the targets are selected at phases earlier than  $\sim -14$  days, it is likely that an observing strategy with a time delay greater than 7 days would yield a higher number of SN spectra with a  $\text{SNR}_{15\text{\AA}} > 5$ . However, such an observing strategy would be counterproductive for our YSN selection criteria, which aims to provide early SN triggers to allow for early-time spectroscopic observations and thus early-time SN science.

Although we previously stated that the 4MOST observing strategy with a 1 day delay is the most optimal strategy for capitalising on our YSN criteria, this strategy produces the lowest percentage of SNe that have good quality spectra ( $\text{SNR}_{15\text{\AA}} > 5$ ). The most optimal strategy for obtaining the most good quality spectra is the strategy that adopts a 7 day time delay, which obtains 11.5 percent more WFD SN spectra. However, such an observing strategy is not optimal for obtaining YSN spectra. Assuming that the YSN criteria selects the SN 2 days after explosion, the earliest a spectrum could be obtained is 9 days after explosion. This is a considerable amount of time, within which there is valuable information regarding the outer most ejecta layers of a SN that cannot be obtained under this observing strategy. Using a 1 day delayed strategy would provide a much quicker follow-up, allowing for the observation of a SN spectrum as early as 3 days after explosion. Although this strategy produces less good quality spectra, the percentage of good quality spectra obtained is still relatively high at 77.4 percent. Therefore, the 4MOST observing strategy that follows LSST with a 1 day delay is most optimal for TiDES to be able to fully capitalise on our YSN selection criteria for conducting early-time science.

## 5 CONCLUSIONS

We have developed a set of selection criteria specifically for TiDES that will select YSNs from the LSST live transient alerts for spectroscopic follow-up with 4MOST. The aim of our selection criteria was to enhance the TiDES YSN sample by triggering on transient events

sooner than the current TiDES (CF) selection criteria, potentially allowing for observations of SN spectra at earlier phases.

To develop our selection criteria, we first utilised the live transient alerts from ZTF, allowing us to develop a set of selection criteria that could produce a sample of YSN (pre-peak SNe at the time of selection) that was not overly contaminated with post-peak SNe, non-SN transients, and spurious transient alerts. By applying our selection criteria to the ZTF alerts over a period of 71 nights, we produced a YSN sample consisting of 79 classified pre-peak SNe, 112 unclassified but likely pre-peak SNe, and 73 contaminants. The purity of our produced ZTF YSN sample was  $\sim 72$  percent.

To evaluate the effect that our selection criteria could have on the TiDES SN survey, we exploited the latest LSST simulations, producing an LSST YSN sample by applying the following ZTF developed YSN selection criteria:

- (i) Consider only LSST *griz*-bands.
- (ii) Object is brighter than 22.5 mag in any *griz*-bands.
- (iii) Object's declination is between  $5^\circ$  and  $-70^\circ$ .
- (iv) Object's Galactic latitude is not between  $-10^\circ$  and  $10^\circ$ .
- (v) Object has two or more  $> 5\sigma$  detections in a given filter.
- (vi) Object has no previous detections more than 14 days before the latest detection.
- (vii) Brightening rate in any *griz*-band  $> 0.2$  mag/day.

In total our YSN selection criteria produced a LSST selected SN sample consisting of 67388 WFD survey transients and 1167 DDF survey transients. Although this sample is significantly smaller than the CF sample, our selection criteria were developed to select early transients rather than produce a large sample, and is intended to be applied in conjunction to the current TiDES (CF) selection criteria (CF). We demonstrated that our YSN selection criteria can provide early triggers on LSST observed SNe, allowing TiDES to enhance its early SN science capabilities.

In addition, we also showed that our selection criteria is capable of producing a YSN sample that is sufficiently pure. By extrapolating the contamination ratio from the ZTF sample (28 percent) and estimating the maximum possible number of SNe that TiDES could observe over its lifetime, we estimated that 4063 fibre hours (1.6 percent of TiDES's total fibre hours) will be wasted over the 5 year survey. We believe that the number of fibre hours spent on non-SN sources is low enough such that it will not have a significant negative impact on the TiDES survey, especially when considering the early triggering benefit that is gained by our YSN selection criteria.

Finally, we investigated different 4MOST observing strategies to optimise the output of the TiDES survey and our YSN criteria. Specifically, we investigated simplistic 4MOST observing strategies that follow the strategy of LSST with delays of 1, 3, 5, and 7 days, looking only at the LSST WFD fields as 4MOST will apply its own cadence based observing strategy in its DDFs. For the CF sample, our results showed that the 3 day delayed 4MOST strategy was the most optimal strategy, as it provided the highest number of spectra (51.5 percent of observed WFD SNe) that can be reliably classified ( $\text{SNR}_{15\text{\AA}} > 5$ ). However, this was not replicated for the YSN sample, as the 7 day delayed strategy provided the most spectra that can be reliably classified. We did not consider the 7 day delayed 4MOST strategy to be optimal for the YSN sample due to the relatively long delay, which would counteract the early SN triggers. Instead, we considered the 1 day delayed strategy to be the most optimal strategy for the YSN sample, as it provides the quickest follow-up. Although we showed that this strategy produced the lowest percentage of good quality spectra (spectra with a  $\text{SNR}_{15\text{\AA}} > 5$ ), the percentage of good quality spectra is still relatively high at 77.4 percent. Therefore, the

4MOST observing strategy that follows the LSST strategy with a 1 day delay is most optimal for the YSN sample and the resulting early-time SN science.

In summary, this work has demonstrated the benefits that the TiDES survey can gain by implementing our YSN selection criteria along side its own selection criteria. Specifically, we have shown that our YSN criteria will enhance the early-time science capabilities of the TiDES survey. Furthermore, we recommend that future work towards designing and simulating the 4MOST observing strategy should adopt a strategy that closely follows the LSST strategy with a delay of 3 days or a delay of 1 day for optimising the CF sample or the YSN respectively.

## ACKNOWLEDGEMENTS

The authors thank Mathew Smith for their assistance with the simulations, Mark Sullivan for discussions and comments on earlier drafts of this work, and Alexander Fritz for their comments. Extensive use of Python was used during this work, specifically the packages: NumPy (Harris et al. 2020), Astropy (Astropy Collaboration et al. 2013, 2018, 2022), and Matplotlib (Hunter 2007). This work was supported by the Science and Technology Facilities Council (STFC) grant ST/X508810/1. KM acknowledges funding from EU H2020 ERC grant no. 758638 and Horizon Europe ERC grant no. 101125877. IH acknowledges support from STFC through grants ST/Y001230/1 and ST/V000713/1, and a Leverhulme Trust International Fellowship, reference IF-2023-027. SJS acknowledges funding from STFC grants ST/Y001605/1, ST/X006506/1, ST/T000198/1, a Royal Society Research Professorship and the Hintze Charitable Foundation.

## DATA AVAILABILITY

All data are available upon reasonable request to the corresponding author.

## REFERENCES

Astropy Collaboration et al., 2013, *A&A*, **558**, A33  
 Astropy Collaboration et al., 2018, *AJ*, **156**, 123  
 Astropy Collaboration et al., 2022, *ApJ*, **935**, 167  
 Ballard C., et al., 2009, *A&A*, **507**, 85  
 Barbary K., et al., 2024, *SNCosmo*, <https://github.com/sncosmo/sncosmo>, doi:10.5281/zenodo.592747  
 Bellm E. C., et al., 2018, *Publications of the Astronomical Society of the Pacific*, **131**, 018002  
 Ben-Ami S., Konidaris N., Quimby R., Davis J. T., Ngeow C. C., Ritter A., Rudy A., 2012, in McLean I. S., Ramsay S. K., Takami H., eds, *Society of Photo-Optical Instrumentation Engineers (SPIE) Conference Series Vol. 8446, Ground-based and Airborne Instrumentation for Astronomy IV*. p. 844686, doi:10.1117/12.926317  
 Blagorodnova N., et al., 2018, *PASP*, **130**, 035003  
 Boos S. J., Townsley D. M., Shen K. J., 2024, *arXiv e-prints*, p. arXiv:2401.08011  
 Deckers M., et al., 2022, *Monthly Notices of the Royal Astronomical Society*, **512**, 1317  
 Dong Y., et al., 2023, *SN 2022cerv: Iib, Or Not Iib: That Is the Question* (arxiv:2309.09433)  
 Fink M., Hillebrandt, W. Röpke, F. K. 2007, *A&A*, **476**, 1133  
 Fink M., Röpke, F. K. Hillebrandt, W. Seitzzahl, I. R. Sim, S. A. Kromer, M. 2010, *A&A*, **514**, A53

Firth R. E., et al., 2014, *Monthly Notices of the Royal Astronomical Society*, **446**, 3895  
 Fitzpatrick E. L., 1999, *PASP*, **111**, 63  
 Folatelli G., et al., 2006, *The Astrophysical Journal*, **641**, 1039  
 Fremling C., et al., 2020, *ApJ*, **895**, 32  
 Frohmaier C., et al., In Preparation, *TiDES – The 4MOST Time Domain Extragalactic Survey*  
 Gagliano A., et al., 2022, *The Astrophysical Journal*, **924**, 55  
 Ganeshalingam M., Li W., Filippenko A. V., 2011, *Monthly Notices of the Royal Astronomical Society*, **416**, 2607  
 Guiglion G., et al., 2019, *The Messenger*, **175**, 17  
 Hallakoun N., Maoz D., 2019, *MNRAS*, **490**, 657  
 Harris C. R., et al., 2020, *Nature*, **585**, 357  
 Hayden B. T., et al., 2010, *The Astrophysical Journal*, **712**, 350  
 Hounsell R., et al., 2018, *ApJ*, **867**, 23  
 Hunter J. D., 2007, *Computing in Science & Engineering*, **9**, 90  
 IAU 2023, *Transient Name Server*, Available at <https://www.wis-tns.org/> (20/10/2023)  
 Iben I. J., Tutukov A. V., 1984, *ApJ*, **284**, 719  
 Ivezić Ž., LSST Science Collaboration 2018, *The LSST System Science Requirements Document*, Available at <https://docushare.lsst.org/docushare/dsweb/Get/LPM-17> (26/03/2023)  
 Ivezić Ž., et al., 2019, *ApJ*, **873**, 111  
 Kasen D., 2009, *The Astrophysical Journal*, **708**, 1025  
 Kessler R., et al., 2009, *PASP*, **121**, 1028  
 Kozyreva A., Klencki J., Filippenko A. V., Baklanov P., Mironov A., Justham S., Chiavassa A., 2022, *The Astrophysical Journal Letters*, **934**, L31  
 Kromer M., Sim S. A., Fink M., Röpke F. K., Seitzzahl I. R., Hillebrandt W., 2010, *The Astrophysical Journal*, **719**, 1067  
 Kushnir D., Katz B., Dong S., Livne E., Fernández R., 2013, *The Astrophysical Journal Letters*, **778**, L37  
 Magee M. R., Maguire K., Kotak R., Sim S. A., 2021, *MNRAS*, **502**, 3533  
 Masci F. J., et al., 2018, *Publications of the Astronomical Society of the Pacific*, **131**, 018003  
 Milligan A., Hook I., In Preparation, *Testing and Combining Transient Spectral Classification Tools on 4MOST-like Blended Spectra*  
 Noebauer U. M., Kromer M., Taubenberger S., Baklanov P., Blinnikov S., Sorokina E., Hillebrandt W., 2017, *Monthly Notices of the Royal Astronomical Society*, **472**, 2787  
 Ogawa M., Maeda K., Kawabata M., 2023, *The Astrophysical Journal*, **955**, 49  
 Pastorello A., et al., 2007, *Nature*, **447**, 829  
 Patterson M. T., et al., 2018, *Publications of the Astronomical Society of the Pacific*, **131**, 018001  
 Piro A. L., Morozova V. S., 2016, *The Astrophysical Journal*, **826**, 96  
 Polin A., Nugent P., Kasen D., 2019, *The Astrophysical Journal*, **873**, 84  
 Riess A. G., et al., 1999, *The Astronomical Journal*, **118**, 2675  
 Rigault M., et al., 2019, *A&A*, **627**, A115  
 Shen K. J., Moore K., 2014, *The Astrophysical Journal*, **797**, 46  
 Smith N., et al., 2007, *ApJ*, **666**, 1116  
 Smith K. W., et al., 2019, *Research Notes of the AAS*, **3**, 26  
 Smith N., Pearson J., Sand D. J., Ilyin I., Bostroem K. A., Hosseinzadeh G., Shrestha M., 2023, *ApJ*, **956**, 46  
 Soker N., 2011, *Proceedings of the International Astronomical Union*, **7**, 72–75  
 Stefano R. D., Voss R., Claeys J. S. W., 2011, *The Astrophysical Journal Letters*, **738**, L1  
 Swann E., et al., 2019, *The Messenger*, **175**, 58  
 Vincenzi M., Sullivan M., Firth R. E., Gutiérrez C. P., Frohmaier C., Smith M., Angus C., Nichol R. C., 2019, *Monthly Notices of the Royal Astronomical Society*, **489**, 5802  
 Wang B., Zhou W.-H., Zuo Z.-Y., Li Y.-B., Luo X., Zhang J.-J., Liu D.-D., Wu C.-Y., 2016, *Monthly Notices of the Royal Astronomical Society*, **464**, 3965  
 Whelan J., Iben Icko J., 1973, *ApJ*, **186**, 1007  
 Williams R. D., Francis G. P., Lawrence A., Sloan T. M., Smartt S. J., Smith K. W., Young D. R., 2024, *RAS Techniques and Instruments*, **3**, 362  
 Young D. R., 2023, *Sherlock*. Contextual classification of astronomical tran-

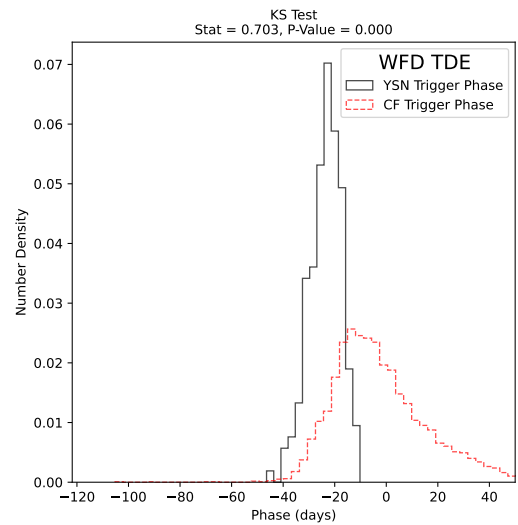
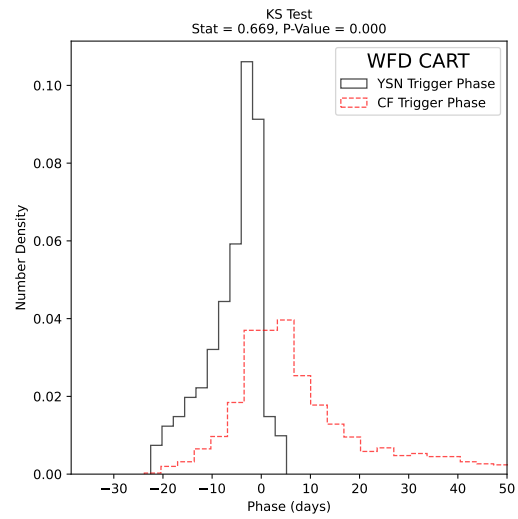
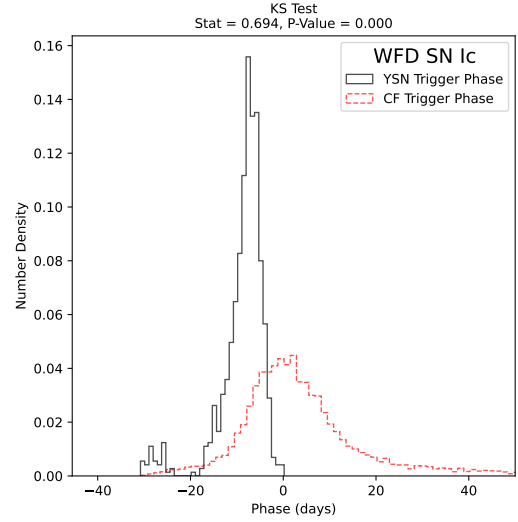
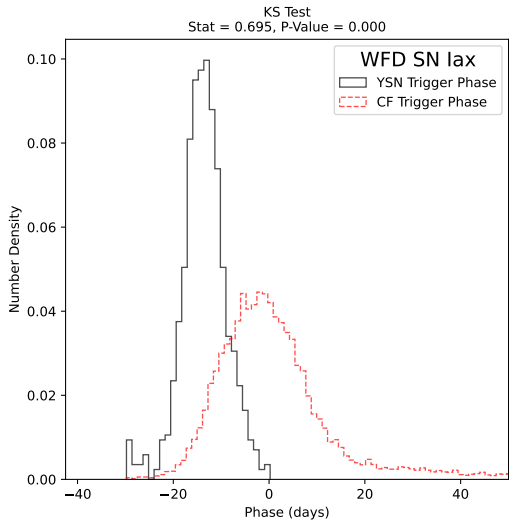
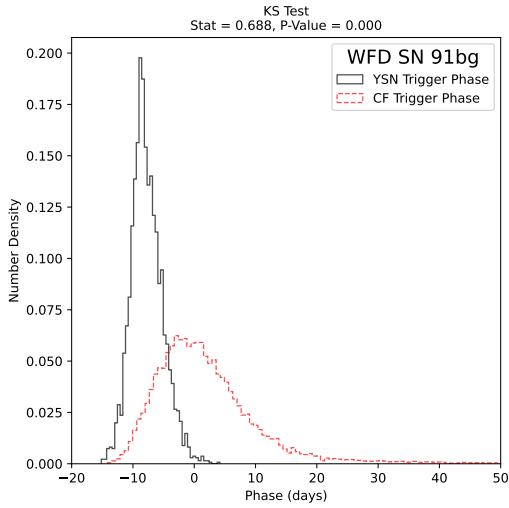
sient sources, [doi:10.5281/zenodo.8038057](https://doi.org/10.5281/zenodo.8038057), <https://zenodo.org/doi/10.5281/zenodo.8038057>

Zimmerman E. A., et al., 2024, *Nature*, 627, 759

de Jong R. S., et al., 2019, *The Messenger*, 175, 3

### APPENDIX A: LSST WFD TRIGGER PHASE DISTRIBUTIONS

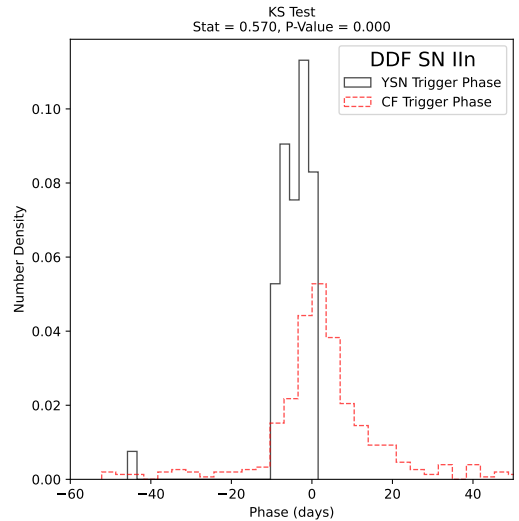
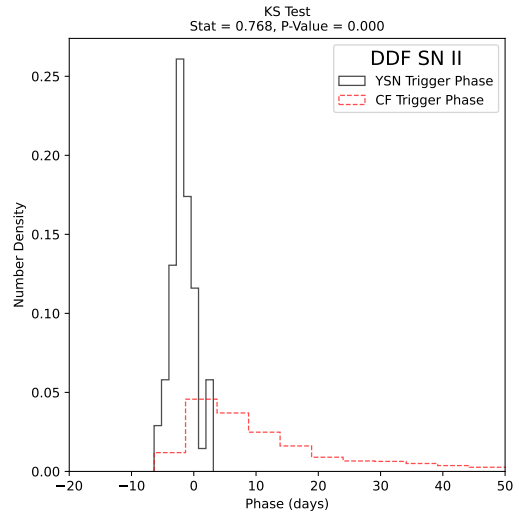
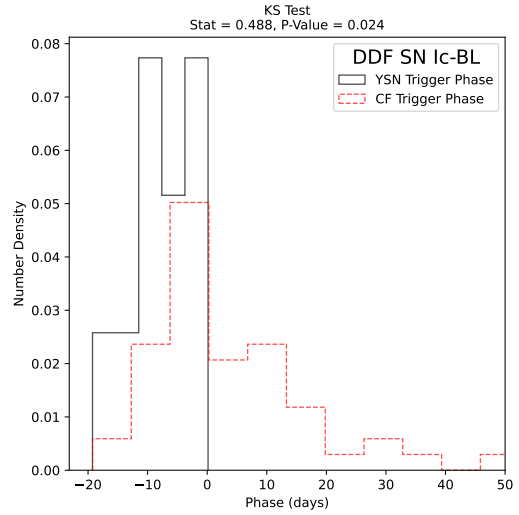
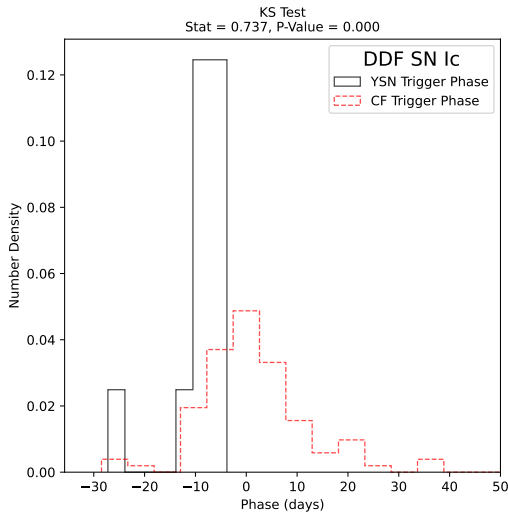
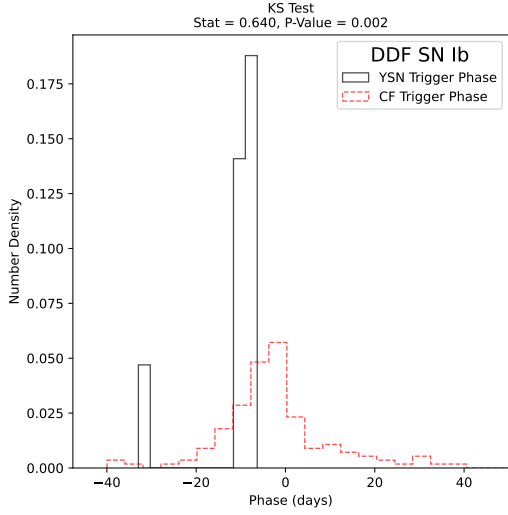
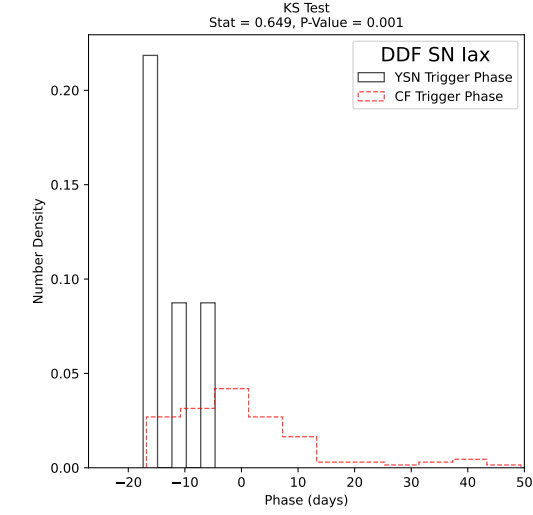
Presented are the WFD survey transients' trigger phase distributions produced by applying our YSN selection criteria and the CF selection criteria to the simulated LSST WFD survey. Only the transient classes not presented in the main body are included here. Note that phases have been truncated at 50 days.

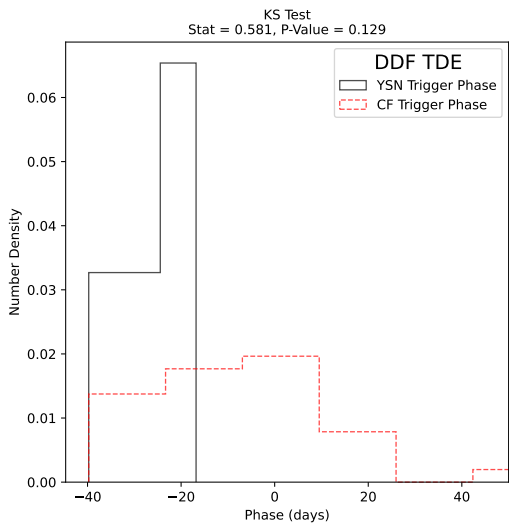
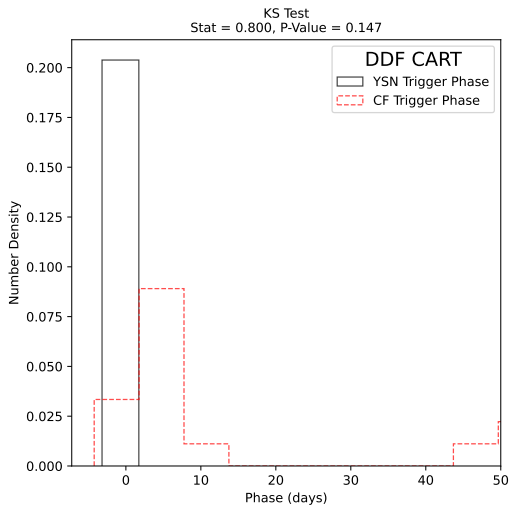
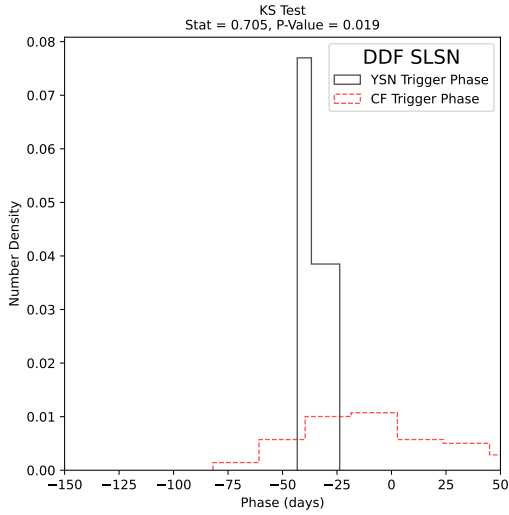


### APPENDIX B: LSST DDF TRIGGER PHASE DISTRIBUTIONS

Presented are the DDF survey transients' trigger phase distributions produced by applying our YSN selection criteria and the CF selection

criteria to the simulated LSST DDF survey. Only the transient classes not presented in the main body are included here. Note that phases have been truncated at 50 days.





This paper has been typeset from a  $\text{\LaTeX}$  file prepared by the author.